



Reverse Engineering the SR-71 Blackbird: Flight Stability and Control, and Synthesis

**Signatures:**

	Name:	Signature:	Dept.:	Date:
Author:	Gayathri Kola		MAE	3/19/2023
Seen:	Dr. Bernd Chudoba		MAE	

**Summary:**

Aircraft conceptual design is the first step in the design process. It is the foremost planning and evaluation stage that creates a design for a specific purpose. Understanding all aspects of aircraft design is essential to come up with creative yet feasible concepts. This year's Aerospace Engineering senior design course aims to teach students the conceptual design process through the reverse engineering of the SR-71 Blackbird. The iconic Intelligence, Stealth, and Reconnaissance aircraft's design was ahead of its time when introduced back in the 1960s. This high-altitude, long-range, high-speed aircraft was capable of flying at Mach 3+ for hours in the air. This capstone project aims to redesign this aircraft using a sizing methodology known as Hypersonic Convergence. Various sizing methods are evaluated first and compared for pros and cons. A mission profile is created for the flight for a payload of 3000 lb, single pilot using Pratt & Whitney J58 Turbo-Ramjet engines. A total of 9 students work on this project with 7 disciplines. Each student must be responsible for a primary and secondary discipline of the design process. Weekly progress reports are written by the students to record their understanding and findings.

The aircraft conceptual design is split into three sub-phases: Parametric Sizing (PS), Configuration Layout (CL), and Configuration Evaluation (CE). The PS stage utilizes the Hypersonic Convergence methodology to size the vehicle based chosen gross configurations for the vehicle synthesis. For Stability and Control of the aircraft, the control surfaces are sized to meet the flight authority requirements which are further verified using the SR-71 Flight Manual.

**Distribution:**

Institution:	Dept.:	Name:
The University of Texas at Arlington	MAE	Dr. Bernd Chudoba

 <b>PENGUIN SUPersonic</b>	SENIOR DESIGN: MAE 4351 Project	Ref.: MAE 4351-001-2021 Date: 19. Mar. 2023 Name: <b>Gayathri Kola</b> Status: In Progress
---	------------------------------------	---

### Work Disclosure Statement

The work I performed to document the results presented in this report was performed by me, or it is otherwise acknowledged.

**Date:** 3/19/2023

**Signature:**





## Table of Contents

<b>WORK DISCLOSURE STATEMENT .....</b>	<b>2</b>
<b>LIST OF FIGURES.....</b>	<b>5</b>
<b>LIST OF TABLES.....</b>	<b>6</b>
<b>NOMENCLATURE .....</b>	<b>7</b>
<i>Greek symbols.....</i>	<b>8</b>
<i>Acronyms .....</i>	<b>8</b>
<b>I. INTRODUCTION .....</b>	<b>9</b>
A. HISTORICAL BACKGROUND.....	<b>9</b>
B. SR-71 BLACKBIRD .....	<b>10</b>
C. PROJECT SCOPE AND MISSION DETAILS.....	<b>11</b>
1. Key Mission Design Parameters.....	<b>11</b>
2. Mission Deliverables .....	<b>11</b>
D. TEAM MANAGEMENT.....	<b>11</b>
1. Team Structure.....	<b>11</b>
2. Team Timeline .....	<b>12</b>
3. Stability and Control Team Structure.....	<b>12</b>
4. Synthesis Team Structure.....	<b>13</b>
<b>II. LITERATURE REVIEW .....</b>	<b>13</b>
A. CONCEPTUAL DESIGN.....	<b>13</b>
1. General Overview.....	<b>14</b>
2. Parametric Sizing .....	<b>14</b>
3. Configuration Layout.....	<b>15</b>
4. Configuration Evaluation .....	<b>15</b>
B. STABILITY AND CONTROL REVIEW.....	<b>15</b>
C. SYNTHESIS REVIEW .....	<b>16</b>
<b>III. INTRA-DISCIPLINARY ANALYSIS (IDA).....</b>	<b>17</b>
A. STABILITY AND CONTROL: IDAS .....	<b>17</b>
B. SYNTHESIS: IDAs.....	<b>18</b>
<b>IV. STABILITY AND CONTROL (S&amp;C).....</b>	<b>19</b>
A. UNDERSTANDING THE DISCIPLINE .....	<b>19</b>
1. John D. Anderson reference [21]: SR-71 Design features .....	<b>19</b>
2. Nicolai [5]: General tailless aircraft methods .....	<b>20</b>
3. SR-71 Flight Manual Reference [22]: Means to verify the methodology .....	<b>21</b>
4. Chudoba [9]: Stability coefficients and previous methodologies .....	<b>22</b>
5. Aircraft Design, A systems engineering approach [27]: Control Surface Sizing .....	<b>23</b>
6. Roskam: Methodology search.....	<b>25</b>
7. USAF DATCOM: Methodology search .....	<b>26</b>
B. METHODOLOGIES .....	<b>26</b>
1. Static and Dynamic Stability.....	<b>26</b>
2. Lateral-Directional Stability.....	<b>27</b>
C. VERIFICATION.....	<b>28</b>
D. CONFIGURATION LAYOUT (CL) .....	<b>28</b>
1. Stability & Control IAO.....	<b>28</b>
2. Vertical fins sizing for directional stability.....	<b>30</b>
3. Elevons sizing for lateral stability. ....	<b>31</b>

 <b>PENGUIN SUPersonic</b>	SENIOR DESIGN: MAE 4351 Project	Ref.: MAE 4351-001-2021 Date: 19. Mar. 2023 Name: <b>Gayathri Kola</b> Status: In Progress
---	------------------------------------	---

<b>E. CONFIGURATION EVALUATION (CE) .....</b>	<b>32</b>
<b>V. SYNTHESIS.....</b>	<b>32</b>
<b>A. UNDERSTANDING THE DISCIPLINE .....</b>	<b>32</b>
1. <i>Reference 1: Roskam [24] .....</i>	<i>32</i>
2. <i>Reference 2: Hypersonic Convergence.....</i>	<i>34</i>
3. <i>Reference 3: AVD Sizing.....</i>	<i>35</i>
<b>B. PARAMETRIC SIZING (PS) .....</b>	<b>36</b>
1. <i>Segregating tasks among disciplines .....</i>	<i>36</i>
2. <i>Estimating Slenderness Ratio (<math>\tau</math>).....</i>	<i>36</i>
3. <i>Trajectory Analysis .....</i>	<i>37</i>
4. <i>Weight and Volume budgets .....</i>	<i>38</i>
<b>C. CONFIGURATION LAYOUT (CL).....</b>	<b>41</b>
<b>VI. CONCLUSION .....</b>	<b>41</b>
<b>APPENDIX .....</b>	<b>41</b>
<b>A. COSTS AND MARKET ESTIMATES APPENDIX .....</b>	<b>41</b>
<b>B. STABILITY AND CONTROL APPENDIX .....</b>	<b>42</b>
<b>C. SYNTHESIS APPENDIX .....</b>	<b>45</b>
<b>ACKNOWLEDGMENTS .....</b>	<b>46</b>
<b>REFERENCES .....</b>	<b>47</b>



## List of Figures

Fig. 1 The SR-71 Blackbird, during its record-breaking flight in 1990 [1].....	9
Fig. 2 The SR-71 Blackbird and its design features [2].....	10
Fig. 3 The SR-71 Reconnaissance Profile [4].....	11
Fig. 4 Team timeline created by Wesley Junell.....	12
Fig. 5 Penguin Supersonic: Updated Team Roster.....	12
Fig. 6 Stability and Control team breakdown.....	13
Fig. 7 New Synthesis team breakdown.....	13
Fig. 8 Aircraft design phases [5].....	14
Fig. 9 Conceptual design phase levels [7].....	14
Fig. 10 Wight and volume budgets for convergence [8].....	15
Fig. 11 Design Team Weekly Meeting Input Categorization.....	15
Fig. 12. IDA for Configuration Layout.....	17
Fig. 13. IDA for Configuration Evaluation [20].....	17
Fig. 14. IDAs for Stability and Control.....	17
Fig. 15 IDA for Synthesis PS Stage [8].....	18
Fig. 16 Neutral point shift from subsonic to supersonic for SR-71 [21].....	19
Fig. 17 Crossflow of streamlines for chines versus a cylindrical fuselage [21].....	20
Fig. 18 Rolling moments of the SR-71 vertical tail with and without canting [21].....	20
Fig. 19 Important non-dimensional parameters and sign convention [5].....	21
Fig. 20 Freebody diagram of forces and moments acting on a tailless aircraft [5].....	21
Fig. 21 Flight geometry data for elevon and vertical tail [22].....	22
Fig. 22 Translational and rotational stability and control derivatives [9].....	23
Fig. 23 Typical vertical tail parameters and geometry [27].....	24
Fig. 24 Control surface design process [27].....	24
Fig. 25 Typical values for static and dynamic stability of an aircraft [27].....	25
Fig. 26 Horizontal tail setting configurations; (a) Fixed, (b) Adjustable, (c) All-moving [27] .....	25
Fig. 27 Vertical fin movement of the SR-71 [28].....	25
Fig. 28 USAF DATCOM stability equations [29].....	26
Fig. 29 MIL-F-8785C Aircraft classes [23].....	27
Fig. 30 Stabilizing and de-stabilizing plots with respect to the angle of attack and sideslip [27] .....	28
Fig. 31 Initial IAO for Stability and Control.....	29
Fig. 32 Detailed IAO by the team lead Austin Prior.....	29
Fig. 33 Parameter breakdown for each phase of Stability and Control [20].....	30
Fig. 34 Rolling moment coefficient $C_{l\beta VT}$ vs. vertical tail area for various vertical c.g. positions.....	31
Fig. 35 Elevon sizing for pitch stability by Noah Blakely.....	31
Fig. 36 Yawing moment as a function of sideslip angle for supersonic Mach numbers.....	32
Fig. 37 Roskam Preliminary Sizing process and Operating Empty Weight estimation [8] .....	33
Fig. 38 An example of a matching point diagram to generate a solution space [6].....	33
Fig. 39 Difference between Hypersonic Convergence and classical sizing logic [8] .....	34
Fig. 40 Hypersonic convergence design point estimation [8].....	35
Fig. 41 AVD sizing logic [8].....	35
Fig. 42 The SR-71 mission profile created by Phat Nguyen.....	36
Fig. 43 The $kw$ as a function of slenderness ratio for various geometries [19].....	36
Fig. 44 Relationship between slenderness ratio and $kw$ [8].....	37
Fig. 45 The $kw$ as a function of slenderness ratio for various configurations by Austin Prior.....	37
Fig. 46 Fuel fractions for different types of aircraft at various mission phases [24] .....	38
Fig. 47 Hypersonic Convergence variables and the relationships [25].....	39
Fig. 48 Coefficient ranges for Weight and Volume Budget equations [32] .....	40
Fig. 49 Geometry change based on solution space geometry by Austin Prior.....	41
Fig. 50 Initial IAO for Costs and Market Estimates.....	42

 <b>PENGUIN SUPersonic</b>	<b>SENIOR DESIGN:</b> <b>MAE 4351 Project</b>	Ref.: MAE 4351-001-2021 Date: 19. Mar. 2023 Name: <b>Gayathri Kola</b> Status: In Progress
---	--	---

## List of Tables

Table 1. Literature Review for Stability and Control .....	15
Table 2. Literature Review for Synthesis. ....	16
Table 3. Important longitudinal and lateral stability derivatives [9].....	22
Table 4. Vertical tail design parameters [27].....	23
Table 5. Lateral-Directional Stability Criteria [5]. .....	27
Table 6. Aircraft similar to SR-71 with delta wings and elevons. ....	28
Table 7. Literature Review for Costs and Market Estimates. ....	41

 <b>PENGUIN SUPersonic</b>	<b>SENIOR DESIGN:</b> <b>MAE 4351 Project</b>	Ref.: MAE 4351-001-2021 Date: 19. Mar. 2023 Name: <b>Gayathri Kola</b> Status: In Progress
---	--	---

## Nomenclature

$x$	= x-axis distance from aircraft center of gravity to wing aerodynamic center
$w$	= mean fuselage width
$Vol$	= fuselage volume
$T$	= engine thrust
$T$	= engine thrust
$M$	= Mach number
$h$	= mean fuselage depth
$d$	= maximum fuselage depth
$b$	= wingspan
$z_w$	= z-axis distance from the wing root to the fuselage centerline
$z_v$	= distance of mean aerodynamic chord of the vertical tail to vertical tail projection
$q_{VT}$	= dynamic pressure of the vertical tail
$q_\infty$	= freestream dynamic pressure
$\dot{m}$	= engine mass flow rate
$l_f$	= distance from side force to center of gravity
$l_e$	= y-axis distance from the fuselage centerline to the engine centerline
$l_{VT}$	= distance from the center of gravity to the vertical tail center of gravity
$c_t$	= wing tip chord
$c_r$	= wing root chord
$\bar{c}$	= mean aerodynamic chord of the wing
$S_{ref}$	= wing planform area
$S_{refVT}$	= reference area of the vertical tail
$L_f$	= side force on the fuselage
$L_{VT}$	= side force on the vertical tail
$D_e$	= engine drag
$C_{n\beta}$	= yawing moment due to side slip angle
$C_{n\beta wing}$	= yawing moment due to the side slip angle of the wing
$C_{n\beta fus}$	= yawing moment due to the side slip angle of the fuselage
$C_L$	= wing lift coefficient
$C_{LaVT}$	= lift curve slope of vertical tail based on the vertical tail planform area
$C_{l\beta wing}$	= rolling moment due to the side slip angle of the wing
$C_{l\beta fus}$	= rolling moment due to the side slip angle of the fuselage
$\bar{V}_{VT}$	= vertical tail coefficient
$C_{l\beta}$	= rolling moment due to side slip angle
$C_{L\alpha}$	= lift coefficient due to the angle of attack
$C_{D\alpha}$	= drag coefficient due to the angle of attack
$C_{m\alpha}$	= pitching moment coefficient due to the angle of attack
$C_{Lq}$	= lift coefficient due to pitch rate
$C_{mq}$	= pitching moment coefficient due to pitch rate
$C_{Y\beta}$	= sideforce coefficient due to the angle of sideslip
$C_{Yp}$	= sideforce coefficient due to roll rate
$C_{lp}$	= rolling moment coefficient due to roll rate
$C_{np}$	= yawing moment coefficient due to roll rate
$C_{Yr}$	= sideforce coefficient due to yaw rate
$C_{lr}$	= rolling moment coefficient due to yaw rate

 <b>PENGUIN SUPersonic</b>	<b>SENIOR DESIGN:</b> <b>MAE 4351 Project</b>	Ref.: MAE 4351-001-2021 Date: 19. Mar. 2023 Name: <b>Gayathri Kola</b> Status: In Progress
---	--	---

$C_{n_r}$  = yawing moment coefficient due to yaw rate

*Greek symbols*

$\Lambda_{c/4}$	= sweep angle at quarter chord
$\delta_a$	= aileron deflection angle
$\delta_e$	= elevator deflection angle
$\delta_r$	= rudder deflection angle
$\Lambda$	= wing sweep angle
$T$	= engine thrust
$T$	= engine thrust
$\alpha$	= angle of attack
$\beta$	= side slip angle

*Acronyms*

<i>a.c.</i>	= aerodynamic center
<i>AR</i>	= Aspect Ratio
<i>c.g.</i>	= center of gravity
<i>CD</i>	= Conceptual Design
<i>CL</i>	= Configuration Layout
<i>DD</i>	= Detailed Design
<i>HTHL</i>	= Horizontal Takeoff and Horizontal Landing
<i>IAO</i>	= Input Analysis Output
<i>IDA</i>	= Individual Disciplinary Analysis
<i>LCC</i>	= Life Cycle Cost
<i>MDA</i>	= Multidisciplinary Analysis
<i>np</i>	= neutral point
<i>O&amp;S</i>	= Operations and Support
<i>PD</i>	= Preliminary Design
<i>PS</i>	= Parametric Sizing
<i>S&amp;C</i>	= Stability and Control
<i>SAS</i>	= Stability Augmentation System
<i>SM</i>	= Static Margin
<i>FH</i>	= Flying Hours
<i>MMH</i>	= Maintenance Man Hours
<i>VLM</i>	= Vortex Lattice Method



## I. Introduction

Since the 1960s, the Soviet Union, the United States, and the European Union have been competing vigorously in making the fastest, deadliest fighter jets and surveillance aircraft mankind has ever seen. This “arms race” as we call it today, has been an ongoing show of a country’s military strength and rate of innovation in the aerospace and defense industry. To date, one such aircraft has captured the attention of many airplane design enthusiasts. The plane is the iconic SR-71 *Blackbird*, a strategic reconnaissance aircraft designed for stealth during the cold war, back in the 1960s. It flew so fast, to date it’s the fastest Horizontal-Takeoff-Horizontal-Landing (HTHL) aircraft ever built. This was a consequence of the many previous iterations created in order to build a strong, undetectable spy plane.



**Fig. 1 The SR-71 Blackbird, during its record-breaking flight in 1990 [1].**

### A. Historical Background

In 1955, the U-2, United States spy plane was shot down by the Soviet Union’s surface-to-air missile, DVINA SA-2 [1]. Until then, the plane was known to reach a high altitude of 70,000 ft which enabled it to escape Russian radars. However, the plane was not as invulnerable as the US government hoped. The plane was already detected by the Soviets, and it was a matter of time before they caught up with deadlier missiles. The need for a special, reconnaissance plane emerged that could stay invisible while it flew along the Soviet Union’s airspace.

Amidst the cold war in 1957, US intelligence obtained news on Soviet Union’s secret Inter-Continental Ballistic Missile development program. This program could hurt US surveillance aircraft like the U-2 with its advanced tracking capabilities. The CIA contracted Lockheed Martin’s Advanced Development Program nicknamed “Skunk Works” for the development of a new, high-speed reconnaissance aircraft, emphasizing a reduced radar signature [2].

This project, led by the infamous aircraft designer, Clarence (Kelly) Johnson was secretly codenamed Archangel. The plane was to replace the U-2 with higher stealth capability, flying to higher altitudes at supersonic speeds. Initially, the design team at Skunk Works produced 11 different designs: A-1 through A-11 [2]. The best design A-10 was chosen by Kelly Johnson to convince the CIA. However, there was one caveat. The plane A-10 would be bigger, and faster, flying at Mach 3.0 but 100% visible to radar. The CIA pushed back on this design and enforced a strong need for an undetectable spy plane. Kelly Johnson and his design team spent the next several months coming up with a new design that combined some of the stealth aspects from previous iterations.

This new design later went on to have three variants. One for the CIA named A-12, one interceptor prototype with armed air-to-air missiles named YF-12 for the Air Force, and lastly, an unmanned reconnaissance drone to be mounted known as the M-21.



## B. SR-71 Blackbird

The aircraft we now call the SR-71 was another US Air Force variant of the highly classified A-12 fleet. To reduce the radar signature, engineers at Lockheed had to modify conventional round fuselage designs.

The new SR-71 had a flattened underbelly. This shape deflected the radar signals away from the plane rather than reflecting them to any radar. Chines were added along the fuselage to prove additional lift and stability [2]. This gave the plane the radar profile of a large bird. To reach high altitudes, the plane has to be lightweight and have high strength to withstand temperatures at Mach 3-plus. In those days, Titanium was the only lightweight material that could withstand such high temperatures at approximately 600°C without melting. Completely new forging, refinement, and manufacturing facilities had to be built to allow for the development of SR-71. This made the program very expensive to operate.

For stability, the plane now had elevons with combined aileron and elevator functionality in a single control surface. A single rudder was replaced by two all-moving vertical fins atop the engine nacelles. These fins were canted inward to further reduce radar cross-section.

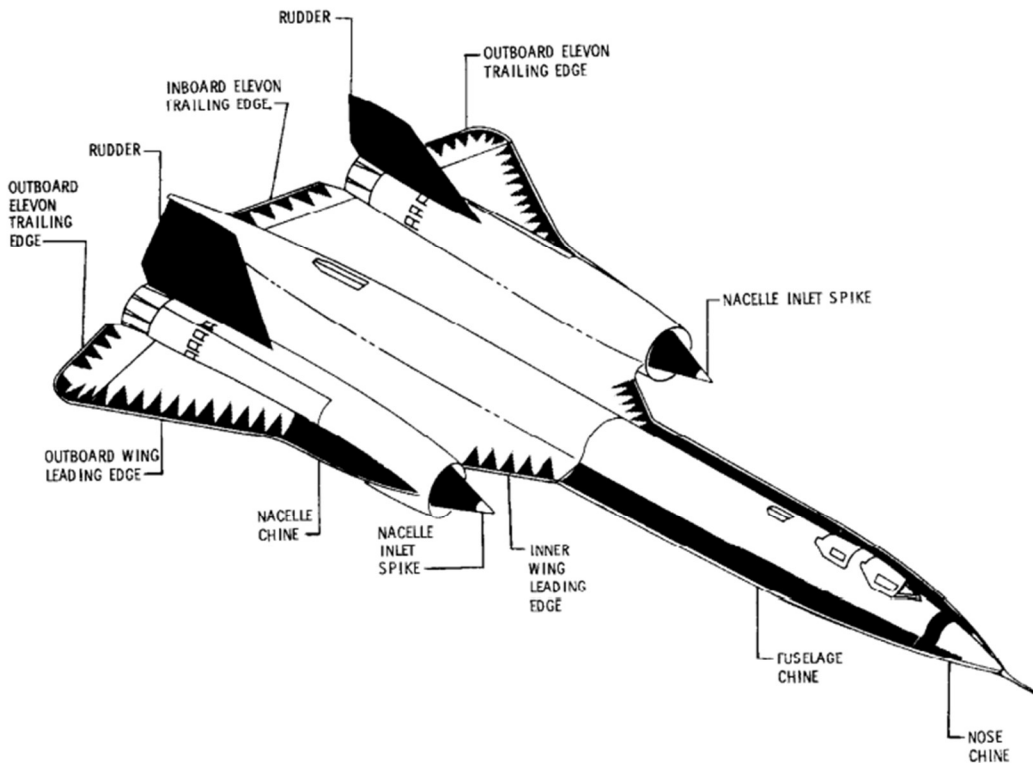


Fig. 2 The SR-71 Blackbird and its design features [2].

To gain more reduction, the wing edges, and control surfaces were made of composite plastic laminates illustrated by triangle patterns in Fig. 2 [2]. Since the plane's main purpose is for surveillance operation, there were no onboard air-to-air missiles, and the extra space was used for storing massive amounts of low volatility fuel named JP-7.

The SR-71 used a dual propulsion system resting in a single-engine nacelle. Its Pratt and Whitney J-58 engines behaved like a conventional turbojet below Mach 2.0, enabling takeoff and landing for the aircraft. Once there was enough forward movement of air at the inlet, the engines switched to a ramjet and bypassed the air straight to the afterburner to cruise at supersonic speeds of Mach 3+.

Although detectable, the aircraft was so fast that it could outmaneuver any missile by simply changing its course or climbing higher. This made the SR-71 invulnerable at its time.



### C. Project Scope and Mission Details

#### 1. Key Mission Design Parameters

Throughout the semester, the team will perform a literature review and record all the progress in the form of individual/midterm reports. The goal is to reverse engineer the SR-71 through synthesis-based design architecture. The geometry is held constant, but other parameters such as material and propulsion system are to be updated to fit the requirements of modern times. A comparison study is to be performed between the original versus modern design. The mission is to design the aircraft to reach a target altitude of 85,000 ft, taking off from the Edwards Air Force Base main runway with a length of 15,024 ft [3].

#### 2. Mission Deliverables

The aircraft must be capable of carrying out both single-legged and multi-legged missions carrying a payload of 3,000 lbs and a single pilot with minimum equipment. For a single-legged mission, the aircraft will have to take off, climb, and fly at a target area for one hour and then land safely. In a multi-legged mission, the aircraft will be refueled mid-air at a lower subsonic altitude multiple times before climbing back to the target altitude, thereby increasing its range. A typical SR-71 mission profile is outlined in Fig. 3Fig. 3Fig. 3Fig. 3Fig. 3. The vehicle has to be capable of performing a Horizontal-Takeoff-Horizontal-Landing (HTHL) at the Edwards Air Force base using the original Pratt & Whitney J-58 (JT11D-20) turbo-ramjet engines.

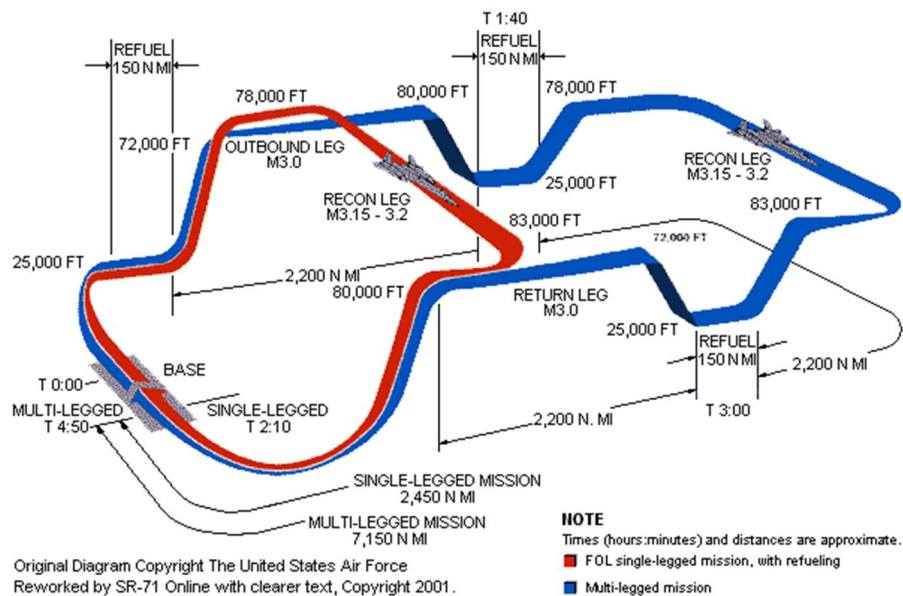


**Fig. 3 The SR-71 Reconnaissance Profile [4].**

### D. Team Management

This semester, our senior design team Penguin Supersonic will be reverse-engineering the SR-71 Blackbird to familiarize ourselves with the conceptual design phase of aircraft design. The focus is to recreate the high-speed, high-altitude, long-range SR-71 through detailed analysis and data comparison.

#### 1. Team Structure

Our team is split into seven divisions, each focusing on different categories of aircraft analysis shown in Fig. 5. The names highlighted in red are the respective team leads. Each team consists of 2-3 engineers, and each chooses a primary and secondary discipline to focus on.

 <b>PENGUIN SUPersonic</b>	<b>SENIOR DESIGN: MAE 4351 Project</b>	Ref.: MAE 4351-001-2021 Date: 19. Mar. 2023 Name: <b>Gayathri Kola</b> Status: In Progress
---	--	---

## 2. Team Timeline

The Fig. 4 shows the tentative team timeline. The majority of the semester will be spent performing a literature review to find convergence methods, and resources to verify these methods.

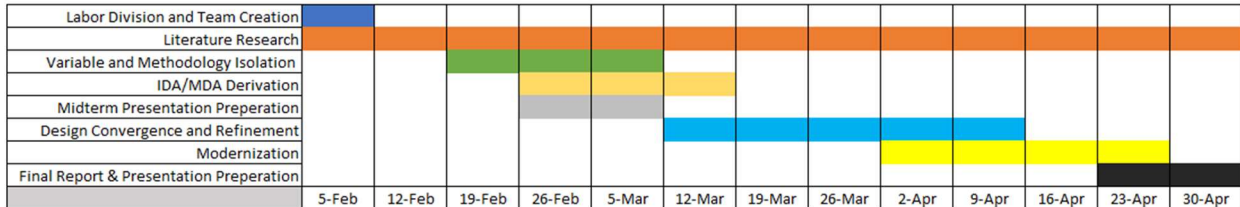


**Fig. 4 Team timeline created by Wesley Junell.**

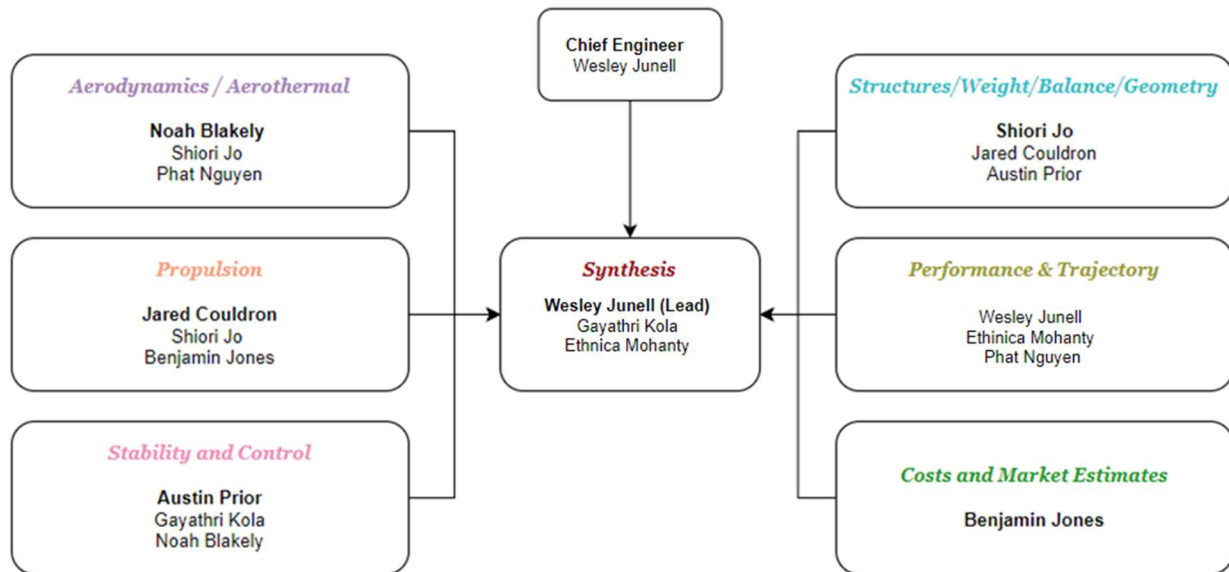


**Fig. 5 Penguin Supersonic: Updated Team Roster.**

This report will primarily focus on two disciplines: Stability and Control, and Cost and Market Estimates of SR-71. This section will elaborate on each of the team's responsibilities, references gathered and reviewed literature. Due to a team member dropping out of the course in week 4, the entire team was restructured. The author of this report has been moved from the Costs team to the Synthesis team, due to the current workload.

## 3. Stability and Control Team Structure

The primary discipline this report will cover is Stability and Control. Within the discipline, each member of our team is individually focusing on three different topics: longitudinal stability, lateral-directional stability, and controls. This report will focus on an attempt to categorize and understand the lateral and directional stability of SR-71. The breakdown of the Stability and Control team is given below in Fig 6, with the names highlighted in blue. The weekly team meetings will occur on Wednesdays.

 <b>PENGUIN SUPERSONIC</b>	<b>SENIOR DESIGN: MAE 4351 Project</b>	Ref.: MAE 4351-001-2021 Date: 19. Mar. 2023 Name: <b>Gayathri Kola</b> Status: In Progress
---	--	---

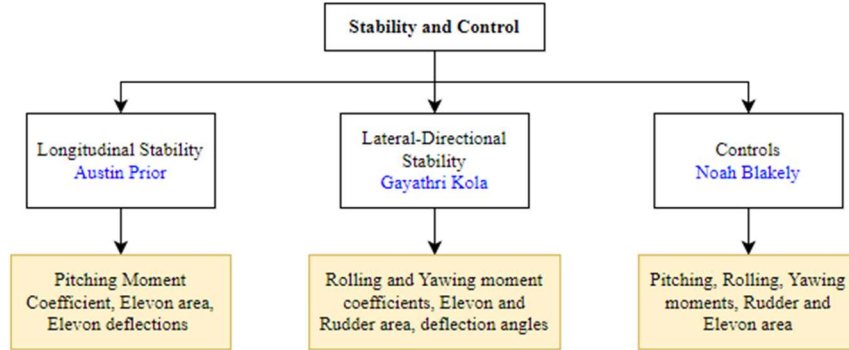


**Fig. 6 Stability and Control team breakdown.**

#### 4. Synthesis Team Structure

The secondary discipline this report will cover is Synthesis. The author has been moved to Synthesis due to a lack of team members needed for the current workload. This team's primary goal is to finalize a sizing method for the Parametric Sizing (PS) stage of the Conceptual Design (CD) phase. The author of this report is responsible for the Configuration Evaluation (CE) phase of CD.

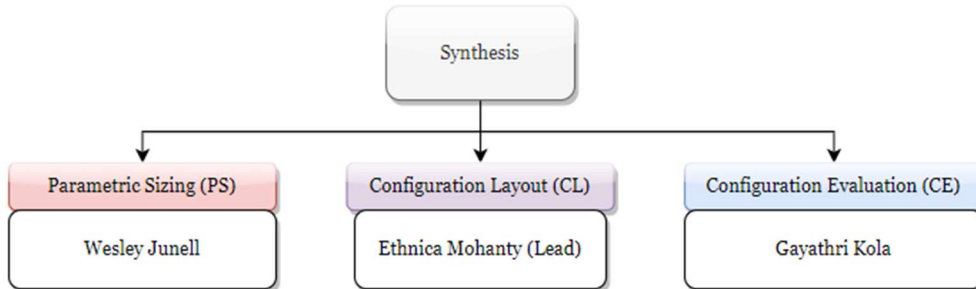


**Fig. 7 New Synthesis team breakdown.**

## II. Literature Review

To start, a literature review is performed amongst all disciplines to identify parameters within the team needed for an Input-Analyse-Output (IAO) formation. The section will briefly cover phases of aircraft design and convergence methodology called “Hypersonic Convergence” being considered by the Synthesis team. This will help in developing a base knowledge for the Costs and Market Estimates team later once the convergence process starts.

### A. Conceptual Design

Once an aircraft company receives an order from a customer or the military, the design team goes through the first step of accessing the feasibility of the concept. This phase of design where a design is generated, and its feasibility is studied by performing important base calculations is called Conceptual Design (CD). A methodology is developed based on all gathered data from various disciplines and a list of all possible designs is generated. This is the first phase of an aircraft design process followed by Preliminary Design (PD) and Detailed Design (DD).

As the names suggest, PD is a more comprehensive analysis through wind tunnel tests. The engines are selected, and structural loads and stresses are determined. Detailed trade studies are performed. In the DD phase, the best design is finalized and sent to shop rooms to be built. Prototype models are fabricated, and the required hardware is identified. Interiors are laid out; blueprints of hydraulic lines are made, and equipment is mounted in place [5].



Phase 1 Conceptual Design		Phase 2 Preliminary Design	Phase 3 Detail Design
<b>Known</b>	Basic Mission Requirements Range, Altitude, & Speed Basic Material Properties $\sigma/p$ $E/p$ $S/lb$	Aeroelastic Requirements Fatigue Requirements Flutter Requirements Overall Strength Requirements	Local Strength Requirements Producibility Functional Requirements
<b>Results</b>	Geometry Airfoil Type R t/c $\lambda$ $\Delta$	Design Objectives Drag Level Weight Goals Cost Goals	Basic Internal Arrangement Complete External Configuration Camber & Twist Distribution Local Flow Problems Solved Major Loads, Stresses, Deflections
<b>Output</b>	Feasible Design	Mature Design	Shop Designs
<b>TRL</b>	2 – 3	4 – 5	6 – 7

Fig. 8 Aircraft design phases [5].

### 1. General Overview

The literature review is performed in an effort to identify all the parameters for deriving IDA/MDA methodologies. The CD phase has three levels – Parametric Sizing (PS), Configuration Layout (CL), and Configuration Evaluation (CE). First, in PS, the feasibility of the mission and the size of the vehicle are determined. Second, in CL, different vehicle configurations are addressed, and trade studies are assessed. Lastly in CE, all the selected design concepts and the trade studies are evaluated at current markets [6].

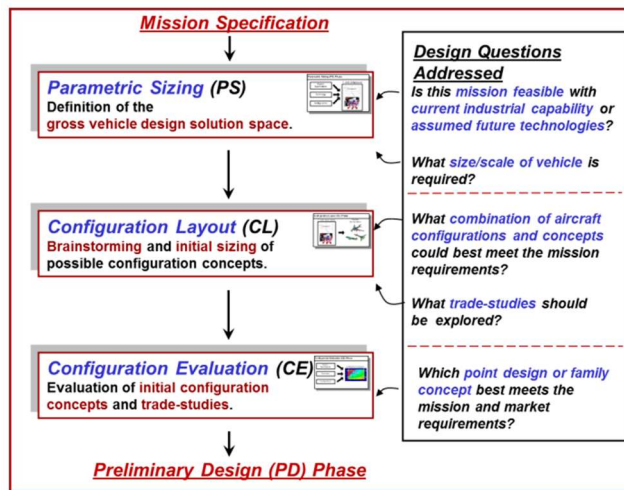


Fig. 9 Conceptual design phase levels [7].

### 2. Parametric Sizing

In Parametric Sizing (PS), a design solution space is identified. This is categorized as physical, technical, and economical. Next, various tools are identified for carrying out sizing. The most commonly known methods are Loftin Sizing, Roskam Sizing, and hypersonic convergence. These are methods the Synthesis team has to choose from for initial sizing. The last step is to obtain deliverables by making plots that aid in solution space visualization. Each discipline will have to make constraint charts, clearly specifying which region is allowable and where it is unacceptable. The synthesis team will weigh all these discipline constraints together to come up with the size and scale of the prospective vehicle [7]. More details on PS will be discussed in the Synthesis section (Section IV).

 <b>PENGUIN SUPERSONIC</b>	<b>SENIOR DESIGN: MAE 4351 Project</b>	Ref.: MAE 4351-001-2021 Date: 19. Mar. 2023 Name: <b>Gayathri Kola</b> Status: In Progress
---	--	---

### 3. Configuration Layout

In Configuration Layout, alternative designs are identified and narrowed down to the solution space. Then, several creative solutions are tested based on available technology, knowledge, and past experience. Lastly, the prioritized technology matrix, configuration trade matrix, and concept trade matrix are made. This phase will generate a list of possible configurations to be evaluated [7].

### 4. Configuration Evaluation

Lastly, in Configuration Evaluation, as the name suggests different configurations are evaluated to come up with a finalized baseline aircraft. Many tools are used such as computer-integrated synthesis, Roskam II, etc.

Once all methodology is set in place for all disciplines, the Synthesis team will perform a convergence analysis of varying key parameters to obtain a *solution space*. A solution space would be a list of feasible designs that fit within the mission criteria. The goal is to obtain the design with the least weight.

**Weight budget**

$$W_{OEW} = \frac{I_{str} K_w S_{pln} + C_{sys} + \frac{(T/W)_{Max} W_R}{E_{TW}} (W_{pay} + W_{crew}) + W_{cprv}}{1 + \mu_a - f_{sys}}$$

Structure      Geometry      Systems      Propulsion      Mission Requirements

**Volume budget**

$$W_{OWE} = \frac{\tau S_{pin}^{1.5} (1 - k_{vv} - k_{vs}) - v_{fix} + N_{crw}(v_{crw} - k_{crw}) - W_{pay}/\rho_{pay}}{\frac{W_R - 1}{\rho_{ppl}} + (k_{ve} (T/W)_{Max} W_R)}$$

Where:

$$W_{OWE} = W_{OEW} + W_{pay} + W_{crew}$$

**Fig. 10 Weight and volume budgets for convergence [8].**

During the second week's design team meeting, an attempt was made to categorize inputs required based on range, altitude, speed, endurance, takeoff, and landing in Fig. 11. The goal is to find relevant references for each level of PS, CL, and CE for each sub-discipline.

	Range	Altitude (85,000 ft)	Speed	Endurance	Takeoff and Landing (Edwards AFB)
<b>Weight Change</b>	✓	✓	✓	✓	✓
<b>Lift-to-Drag Ratio (L/D)</b>	✓		✓	✓	
<b>Vehicle Geometry/ Materials</b>	✓	✓	✓		✓
<b>Thrust Specific Fuel Consumption</b>	✓			✓	
<b>Lift-curve-slope</b>					✓
<b>Propulsion</b>		✓	✓		

**Fig. 11 Design Team Weekly Meeting Input Categorization.**

## B. Stability and Control Review

For the initial references collected, a broad search was performed with keywords such as: 'SR-71', 'Supersonic', 'Stability and Control', 'Trim drag', 'Lateral Stability', 'Airplane Design', etc. Currently, textbooks on stability and control are being reviewed to identify key parameters needed for deriving an Intra-Disciplinary-Analysis/Multi-Disciplinary-Analysis (IDA/MDA) [5,7,18]. Additionally, Table 1 lists all the literature collected so far on this topic.

**Table 1. Literature Review for Stability and Control.**

 <b>PENGUIN SUPersonic</b>	SENIOR DESIGN: MAE 4351 Project	Ref.: MAE 4351-001-2021 Date: 19. Mar. 2023 Name: <b>Gayathri Kola</b> Status: In Progress
---	------------------------------------	---

Serial No.	Title	Author	Year	Category
1	Stability & Control of Conventional & Unconventional Aerospace Vehicle Configurations [9]	Chudoba, B.	2019	Book
2	A Generic Stability and Control Tool for Conceptual Design, Prototype System Overview [10]	Coleman, G. Chudoba, B.	2007	Book Section
3	Airplane Design Part VII: Determination of Stability, Control, and Performance Characteristics [11]	Roskam, J.	2017	Book
4	Design and Development of the Blackbird: Challenges and Lessons Learned [12]	Merlin, P. W.	2009	Conference Paper
5	Stability and Control Estimation Flight Test Results for the SR-71 Aircraft with Externally Mounted Experiments [2]	Moes, T. R.	2002	Book
6	The Lockheed SR-71 Blackbird – A Senior Capstone Re-Engineering Experience [13]	Mixon, B. Chudoba, B.	2007	Book Section
7	Flight Stability and Control and Performance Results from the Linear Aerospike SR-71 Experiment (LASRE) [14]	Moes, T. Et al.	1998	Conference Paper
8	Supersonic Flying Qualities Experience Using the SR-71 [15]	Cox, T. H. Jackson, D.	1997	Conference Paper
9	The SR-71 Test Bed Aircraft: A Facility for High-Speed Flight Research [16]	Corda, S. Et al.	2000	Technical Paper
10	Examination of Recent Lateral-Stability Derivative Data [17]	Malvestuto, F. Kuhn, R. E.	1953	Technical Report
11	Longitudinal Handling Qualities of the Tu-144LL Airplane and Comparisons with Other Large, Supersonic Aircraft [18]	Cox, T. H. Marshall, A.	2000	Journal Article
12	Future Spacecraft Propulsion Systems and Integration: Enabling Technologies for Space Exploration [19]	Czysz, P. Et al.	2018	Book
13	Development of the Vehicle Configuration Compendium: A Comprehensive Data-Information-Knowledge System to Aid in High-Speed Vehicle Design [20]	Simon, S.	2021	Master's Thesis
14	Subsonic Aircraft: Evolution and the Matching of Size to Performance [6]	Loftin, L. K.	1980	Book
15	Fundamentals of Aircraft and Airship Design. Volume I – Aircraft Design [5]	Nicolai, L. M. Carichner, G.	2010	Book
16	Aircraft Performance and Design [21]	Anderson, J.D.	1999	Book
17	Lockheed SR-71 Blackbird: Flight Manual [22]	Kucher, P. R.	2010	Webpages
18	Introduction to Aircraft Flight Mechanics, Performance, Static Stability, Dynamic Stability, and Classical Feedback Control [23]	Yechout, T. R. Et al.	2003	Book

### C. Synthesis Review

Below in Table 2 are the references the author has gathered for the Synthesis literature review. The current focus is to obtain enough information on Parametric Sizing (PS). A lot of progress was made during the team meeting of week 4, and attempts were made to obtain a rough constraint diagram by making plots on MATLAB. More about constraint diagrams and synthesis literature is discussed in section IV.

**Table 2. Literature Review for Synthesis.**

Serial No.	Title	Author	Year	Category
1	Fundamentals of Aircraft and Airship Design. Volume I – Aircraft Design [5]	Nicolai, L. M. Carichner, G.	2010	Book
2	Subsonic Aircraft: Evolution and the Matching of Size to Performance [6]	Loftin, L. K.	1980	Book
3	Development of the Vehicle Configuration Compendium: A Comprehensive Data-Information-Knowledge System to Aid in High-Speed Vehicle Design [20]	Simon, S.	2021	Master's Thesis
4	Future Spacecraft Propulsion Systems and Integration: Enabling Technologies for Space Exploration [19]	Czysz, P. Et al.	2018	Book
5	Hypersonic Convergence: Background and Methodology [8]	Ledford, T. Harris, C.	2023	Guest Lecture
6	Aircraft Design Part I – Preliminary Sizing of Airplanes [24].	Roskam, J.	2012	Series
7	Aircraft Conceptual Design – An Adaptable Parametric Sizing Methodology [25]	Coleman, G.	2010	Thesis
8	Synthesis of Subsonic Airplane Design	Torenbeek, E.	1982	Book
9	General Aviation Aircraft Design: Applied Methods and Procedures [26].	Gudmundsson, S. Czysz, P.	2014 2013	Book Book
10	Scramjet Propulsion: Trans-atmospheric Launcher Sizing			Chapter
11				
12				
13				
14				
15				
16				
17				
18				



### III. Intra-Disciplinary Analysis (IDA)

#### A. Stability and Control: IDAs

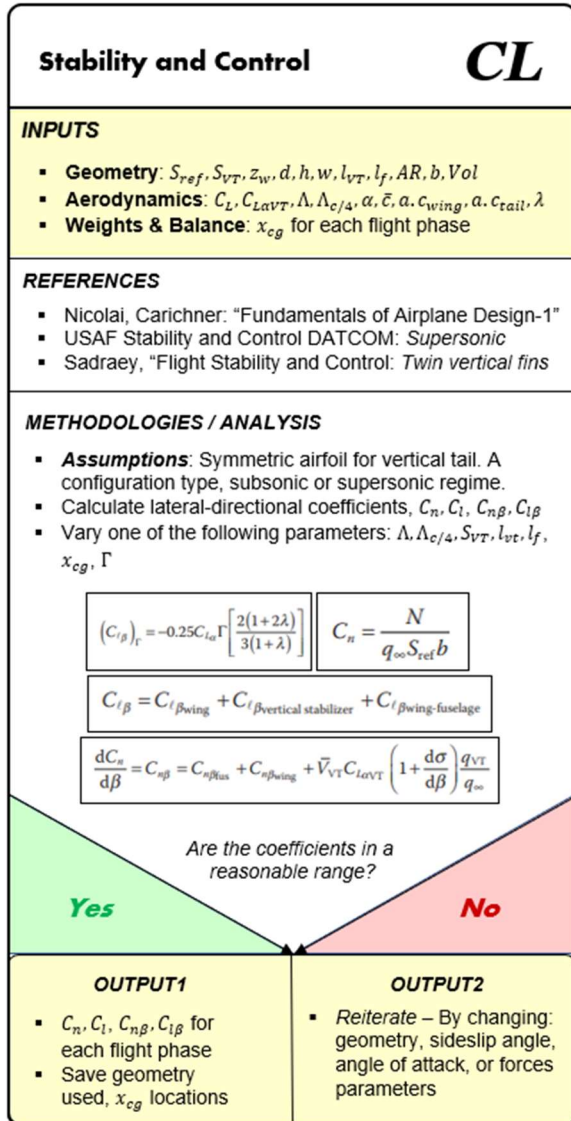


Fig. 12. IDA for Configuration Layout

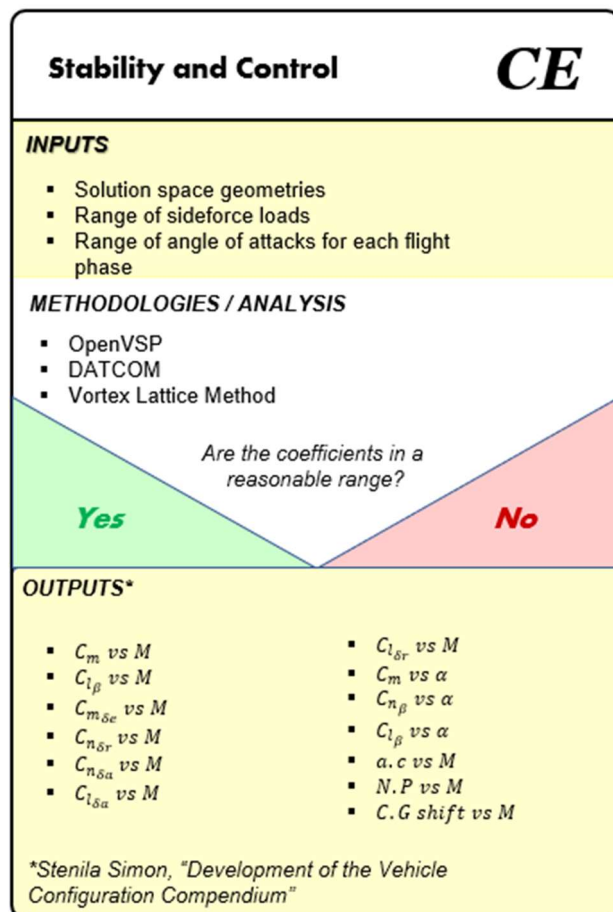


Fig. 13. IDA for Configuration Evaluation [20].

Fig. 14. IDAs for Stability and Control.

 <b>PENGUIN SUPersonic</b>	<b>SENIOR DESIGN:</b> <b>MAE 4351 Project</b>	Ref.: MAE 4351-001-2021 Date: 19. Mar. 2023 Name: <b>Gayathri Kola</b> Status: In Progress
---	--	---

## B. Synthesis: IDAs

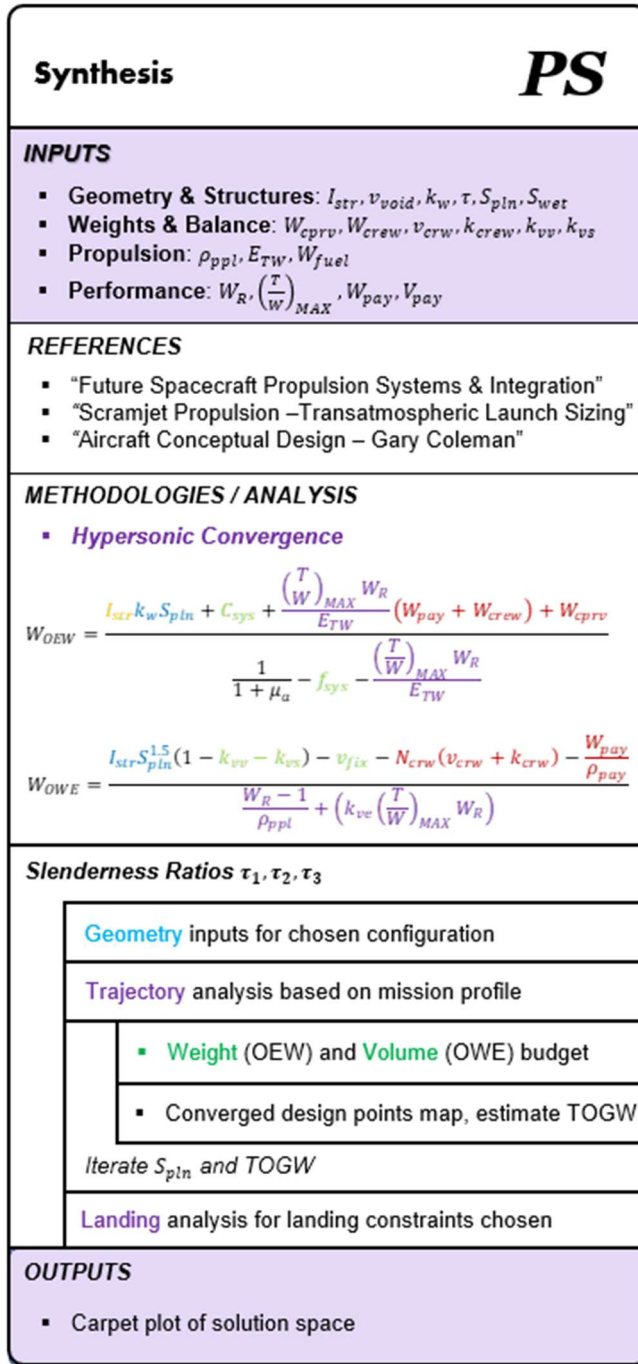


Fig. 15 IDA for Synthesis PS Stage [8].



#### IV. Stability and Control (S&C)

##### A. Understanding the Discipline

In order to get an in-depth understanding of stability and control, three main references are being reviewed initially. For brief descriptions of SR-71 longitudinal and lateral stability features, the textbook “Aircraft Performance and Design” by John D. Anderson was reviewed [21]. To collect input parameters needed from other teams for stability calculations, the course’s main textbook was used [5]. Lastly, to understand the aircraft’s stability characteristics, SR-71’s online flight manual was referenced [22]. In this section, a summary of key elements is given from each reference. The structure of this sub-section will be modified later after reviewing more literature.

###### 1. John D. Anderson reference [21]: SR-71 Design features

Chapter 9 of this text has clear explanations of features like chines that were added to ensure the Blackbird’s stability. The aerodynamic center (neutral point) of an aircraft change substantially when flying from the subsonic to the supersonic regime. This can also be explained from a drag perspective, where the drag coefficient diverges dramatically at sonic speed (Mach 1). These drastic shifts can be a problem for a supersonic aircraft’s pitch stability. Chines, a variation of strakes, reduce the movement of the neutral point as the aircraft travels at supersonic speeds. The Fig. 16 shows the effect of chine as a function of Mach number. The case with chine on brings back the neutral point close to its original location after crossing sonic speed.

According to longitudinal stability criteria, the neutral point of an aircraft must always be behind the center of gravity. This ensures that the aircraft does not pitch up too quickly or enter into high angles of attack that guarantee a stall. This concept is illustrated by the “static margin” in Eq. 1. Where  $X_{np}$  is the location of the neutral point and  $X_{c,g}$  is the center of gravity of the aircraft. A positive SM value means that the neutral point is behind the center of gravity.

$$SM = \frac{X_{np} - X_{c,g}}{\bar{c}} \quad (1)$$

A large positive value indicates that the aircraft is more stable. The faster a plane goes, the farther the neutral point travels from c.g. This causes the plane to become more stable than desired, limiting maneuverability. The elevon will require a higher force to change the vehicle attitude to trim the aircraft. This results in trim drag.

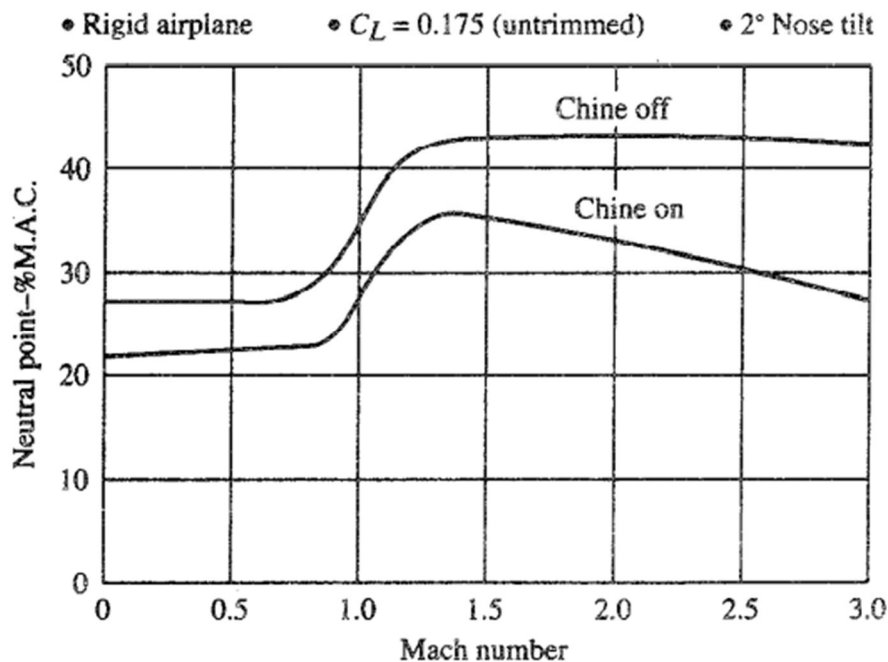


Fig. 16 Neutral point shift from subsonic to supersonic for SR-71 [21].

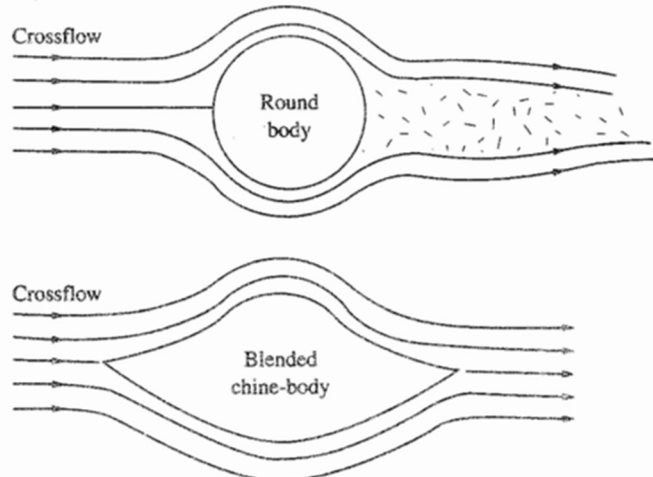


Fig. 17 Crossflow of streamlines for chines versus a cylindrical fuselage [21].

The Fig. 17 above shows the crossflow pattern on a cylindrical fuselage versus a blended-chine body. The crossflow creates a side force on the fuselage that makes it yaw in the flow direction. Cylindrical bodies will experience flow separation for small yaw angles. Having a blended chine as in the case of SR-71 helps a smoother flow resulting in favorable directional stability. This consequently reduces the need for larger vertical tails, thereby reducing weight and skin drag on the aircraft. Chines also aid in producing additional lift. The delta wing was placed at a small negative incidence angle relative to the fuselage centerline due to this.

For directional control, the SR-71 does not have any surfaces. Instead, it is equipped with two all-moving vertical tails that are canted inward by a  $15^\circ$  angle. In the instance of a side force acting on an uncanted vertical tail, the center of pressure for the tail is above the aircraft's longitudinal axis. This caused a rolling moment about the axis, decreasing its lateral stability. By canting the vertical tails, the moment arm is much shorter as seen in Fig. 18. According to the text, the hinges on the rudder surfaces were exposed to high temperatures in supersonic flight tests. They also required large rudder deflection in one engine-out condition. This proved to be very risky in terms of control authority. This was the main reason for using all-moving vertical fins.

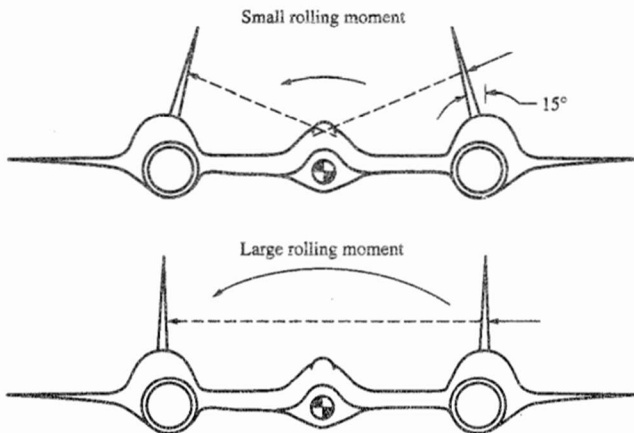


Fig. 18 Rolling moments of the SR-71 vertical tail with and without canting [21].

## 2. Nicolai [5]: General tailless aircraft methods

During week 3, the entire design team decided to use course textbook nomenclature as a standard while performing calculations for convergence. The Fig. 19 shows the Stability and Control team nomenclature to be an aircraft axis system to be adapted. Since Stability and Control will be dealing with forces and moments on the aircraft, the use of



this text helps to establish the various kinds of derivatives involved. Specifically, Chapters 21 – 23 give detailed methods to calculate these moment coefficients, as a starting point. Other methodologies such as Roskam VII which covers step-by-step calculation procedures based on aircraft type will be reviewed in week 4 [11].

Upon reading these chapters, some important equations and parameters were collected in order to derive a draft IDA. The describes methods for longitudinal and lateral stability for different types of control surfaces. The exact equations are discussed further in sub-section C. The SR-71 would be classified as a tailless aircraft since it has no horizontal stabilizer (an aft tail) or canards, only elevons directly attached to the delta wing. As discussed earlier, elevons are responsible for longitudinal (pitch) and lateral (roll) control. Elevons move up and down together to maintain pitch and move in opposite directions to one another to roll. The force-moments diagram is given in Fig. 20.

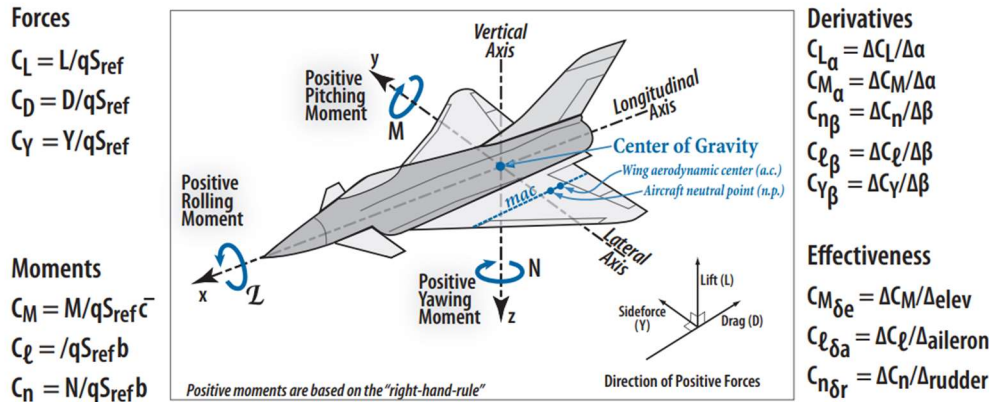
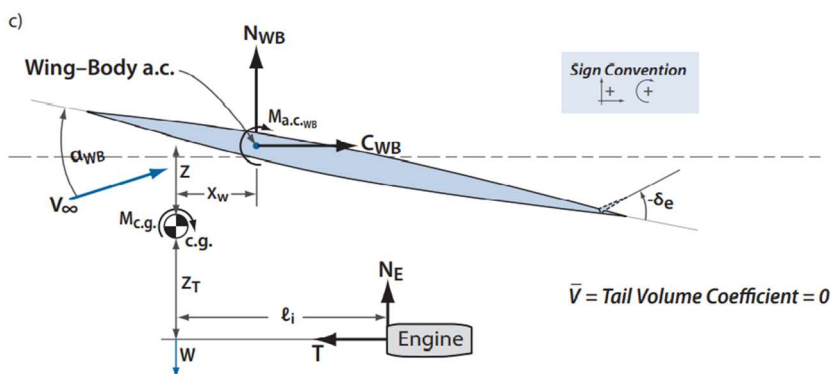


Fig. 19 Important non-dimensional parameters and sign convention [5].



All distances are positive as shown  
 $\epsilon_T$  = tail downwash angle due to wing downwash  $w_T$  at the tail a.c.  
For small  $a$  we can assume  
 $N$  = normal force =  $L = C_L q S_{ref}$   
 $C$  = chord force =  $D = C_D q S_{ref}$

Fig. 20 Freebody diagram of forces and moments acting on a tailless aircraft [5].

There are federal regulations to use as a reference point while making static and dynamic stability criteria in design. Since the SR-71 is a military aircraft, two main documents, MIL-HDBK-1797 and its previous version ML-F-8787C can be referenced. This text outlines some stability criteria from both these documents. The documents state the requirements of aircraft flight operation quality for military aircraft including trans-atmospheric flight where an aircraft uses air-breathing propulsion systems.

### 3. SR-71 Flight Manual Reference [22]: Means to verify the methodology

An estimate of all the control surface area was found in the manual. The Fig. 21 specifies the inboard and outboard elevon areas, movable and total rudder area, and tip and root chords for the wing and vertical tail. These values can



be used to make rough calculations of the different stability derivatives before the Synthesis team gives out this information. Various references use vertical tail and rudders interchangeably while referring to SR-71's directional stabilizer. However, most of them specify "all-moving" to differentiate from conventional rudder-vertical stabilizer combinations.

This flight manual has abundant information on the flight trim system and Stability Augmentation System (SAS) that can be referenced later for method verification purposes.

SR-71 Specifications	
Manufacturer:	Lockheed Aircraft Corporation
Length:	107' 5"
Length of Nose Probe:	4' 11"
Wing Span:	55' 7"
Wing Area:	1,795 ft. sq.
Wing Aspect Ratio:	1.939
Wing Root Chord:	60.533
Wing Dihedral Angle:	0 degrees
Wing Chord:	0.00
Wing Sweep:	52.629 degrees
Inboard Elevon Area:	39.00 ft. sq.
Outboard Elevon Area:	52.50 ft. sq.
Total Vertical Rudder Area:	150.76 ft. sq.
Moveable Rudder Area:	70.24 ft. sq.
Rudder Root Chord:	14.803 ft.
Rudder Tip Chord:	7.833 ft.
Height:	18' 6"
Empty Weight:	59,000 lbs.
Maximum Weight:	170,000 lbs.
Fuselage Diameter:	5.33 ft.
Service Ceiling:	85,000'+
Maximum Speed:	Mach 3.3+ (Limit CIT of 427 degrees C)
Cruising Speed:	Mach 3.2
Engines:	2 Pratt & Whitney J-58 (JT11D-20A) with 34,000 lbs. of thrust.
Range:	3,200 nautical miles (without refueling)

Fig. 21 Flight geometry data for elevon and vertical tail [22]

#### 4. Chudoba [9]: Stability coefficients and previous methodologies

Another methodology, mentioned in the book "Stability and Control of Conventional and Unconventional Aircraft Configurations", known as VORSTAB is a software capable of calculating aerodynamic and stability derivatives using the Vortex Lattice Method (VLM) [9]. This numerical method works for both subsonic and supersonic flow. However, the author has not been able to find this software for free use on the internet.

Another VLM method presented in the same book named VORLAX is also being searched. For now, the current methodology is to write MATLAB scripts to iterate for a range of sideslip angle  $\beta$ , dynamic pressure  $q_\infty$  or Mach number. As a baseline calculation setup, a simplified geometry of the delta wing will be used to obtain the yawing and rolling moment coefficients. This process has to be obtained for each flight phase: takeoff, climb, cruise, descent, approach, loiter, and landing. The Fig. 24 shows a clear control surface design process that can be incorporated. The same book lists all the important stability and control derivatives to consider during the Conceptual Design process – boxed in Fig. 22. The derivatives on the upper side of the table show the stability derivatives and the bottom part lists the control derivatives.

Table 3. Important longitudinal and lateral stability derivatives [9]

Symbol	Parameter Name	Category
$C_{L\alpha}$	Variation of lift coefficient with angle of attack	Longitudinal
$C_{D\alpha}$	Variation of drag coefficient with angle of attack	Longitudinal
$C_{m\alpha}$	Variation of pitching moment coefficient with angle of attack	Longitudinal
$C_{Lq}$	Variation of lift coefficient with pitch rate	Longitudinal
$C_{mq}$	Variation of pitching moment coefficient with pitch rate	Longitudinal
$C_{Y\beta}$	Variation of sideforce coefficient with angle of sideslip	Directional
$C_{l\beta}$	Variation of rolling moment coefficient with angle of sideslip	Lateral
$C_{n\beta}$	Variation of yawing moment coefficient with angle of sideslip	Directional
$C_{Yp}$	Variation of sideforce coefficient with roll rate	Lateral
$C_{lp}$	Variation of rolling moment coefficient with roll rate	Lateral
$C_{np}$	Variation of yawing moment coefficient with roll rate	Lateral



$C_{Y_r}$	Variation of sideforce coefficient with yaw rate	Directional
$C_{l_r}$	Variation of rolling moment coefficient with yaw rate	Directional
$C_{n_r}$	Variation of yawing moment coefficient with yaw rate	Directional

**TABLE 4-7. Matrix of Translational and Rotary Stability Derivative Coefficients**

	X[D,T]	Y	Z[L,W]	L	M	N
$u$	$C_{D_u} C_{T_u}$	$C_{Y_u}$	$C_{L_u}$	$C_{l_u}$	$C_{m_u}$	$C_{n_u}$
$v [\beta]$	$C_{D_\beta} C_{T_\beta}$	$C_{Y_\beta}$	$C_{L_\beta}$	$C_{l_\beta}$	$C_{m_\beta}$	$C_{n_\beta}$
$w [\alpha]$	$C_{D_\alpha} C_{T_\alpha}$	$C_{Y_\alpha}$	$C_{L_\alpha}$	$C_{l_\alpha}$	$C_{m_\alpha}$	$C_{n_\alpha}$
$p$	$C_{D_p} C_{T_p}$	$C_{Y_p}$	$C_{L_p}$	$C_{l_p}$	$C_{m_p}$	$C_{n_p}$
$q$	$C_{D_q} C_{T_q}$	$C_{Y_q}$	$C_{L_q}$	$C_{l_q}$	$C_{m_q}$	$C_{n_q}$
$r$	$C_{D_r} C_{T_r}$	$C_{Y_r}$	$C_{L_r}$	$C_{l_r}$	$C_{m_r}$	$C_{n_r}$
$\dot{u}$	$C_{D_{\dot{u}}} C_{T_{\dot{u}}}$	$C_{Y_{\dot{u}}}$	$C_{L_{\dot{u}}}$	$C_{l_{\dot{u}}}$	$C_{m_{\dot{u}}}$	$C_{n_{\dot{u}}}$
$\dot{v} [\dot{\beta}]$	$C_{D_{\dot{\beta}}} C_{T_{\dot{\beta}}}$	$C_{Y_{\dot{\beta}}}$	$C_{L_{\dot{\beta}}}$	$C_{l_{\dot{\beta}}}$	$C_{m_{\dot{\beta}}}$	$C_{n_{\dot{\beta}}}$
$\dot{w} [\dot{\alpha}]$	$C_{D_{\dot{\alpha}}} C_{T_{\dot{\alpha}}}$	$C_{Y_{\dot{\alpha}}}$	$C_{L_{\dot{\alpha}}}$	$C_{l_{\dot{\alpha}}}$	$C_{m_{\dot{\alpha}}}$	$C_{n_{\dot{\alpha}}}$
$\dot{p}$	$C_{D_p} C_{T_p}$	$C_{Y_p}$	$C_{L_p}$	$C_{l_p}$	$C_{m_p}$	$C_{n_p}$
$\dot{q}$	$C_{D_q} C_{T_q}$	$C_{Y_q}$	$C_{L_q}$	$C_{l_q}$	$C_{m_q}$	$C_{n_q}$
$\dot{r}$	$C_{D_r} C_{T_r}$	$C_{Y_r}$	$C_{L_r}$	$C_{l_r}$	$C_{m_r}$	$C_{n_r}$
$\delta p C_i$	$C_{D_{\delta_{LoCE_i}}} C_{T_{\delta_{LoCE_i}}}$	$C_{Y_{\delta_{LoCE_i}}}$	$C_{L_{\delta_{LoCE_i}}}$	$C_{l_{\delta_{LoCE_i}}}$	$C_{m_{\delta_{LoCE_i}}}$	$C_{n_{\delta_{LoCE_i}}}$
	$C_{D_{\delta_{DiCE_i}}} C_{T_{\delta_{DiCE_i}}}$	$C_{Y_{\delta_{DiCE_i}}}$	$C_{L_{\delta_{DiCE_i}}}$	$C_{l_{\delta_{DiCE_i}}}$	$C_{m_{\delta_{DiCE_i}}}$	$C_{n_{\delta_{DiCE_i}}}$
	$C_{D_{\delta_{LaCE_i}}} C_{T_{\delta_{LaCE_i}}}$	$C_{Y_{\delta_{LaCE_i}}}$	$C_{L_{\delta_{LaCE_i}}}$	$C_{l_{\delta_{LaCE_i}}}$	$C_{m_{\delta_{LaCE_i}}}$	$C_{n_{\delta_{LaCE_i}}}$
$\delta s C_i$	$C_{D_{\delta S_i}} C_{T_{\delta S_i}}$	$C_{Y_{\delta S_i}}$	$C_{L_{\delta S_i}}$	$C_{l_{\delta S_i}}$	$C_{m_{\delta S_i}}$	$C_{n_{\delta S_i}}$
$\delta c S_i$	$C_{D_{\delta CS_i}} C_{T_{\delta CS_i}}$	$C_{Y_{\delta CS_i}}$	$C_{L_{\delta CS_i}}$	$C_{l_{\delta CS_i}}$	$C_{m_{\delta CS_i}}$	$C_{n_{\delta CS_i}}$

**Fig. 22 Translational and rotational stability and control derivatives [9].**

##### 5. Aircraft Design, A systems engineering approach [27]: Control Surface Sizing

This book contains detailed control surface sizing steps, especially for tail design. For a vertical tail design, the book recommends the following parameters shown in Table 4 below.

**Table 4. Vertical tail design parameters [27].**

Symbol	Parameter Name
$S_v$	Tail planform area



$l_v$	Tail arm
$AR_v$	Tail aspect ratio
$\lambda_v$	Tail Taper ratio
$C_{t_v}$	Tail tip chord
$C_{r_v}$	Tail root chord
$MAC_v$ or $C_v$	Mean aerodynamic chord
-	Airfoil section
$b_v$	Tail span
$\Lambda_v$	Tail sweep angle
$\Gamma_v$	Tail dihedral angle
$i_v$	Tail incidence angle

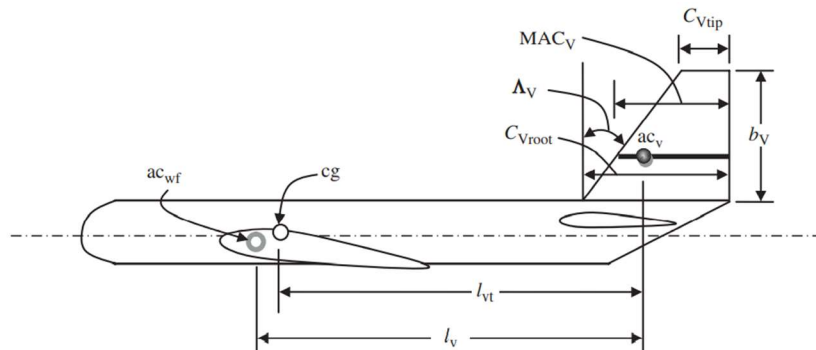


**Fig. 23 Typical vertical tail parameters and geometry [27].**

The Fig. 23 above can be used as a reference for the exact geometry parameters needed for the vertical tail design. Since the SR-71 does not have a horizontal tail, it can be neglected from the design process. The tail design process is very clearly outlined in this book, seen in Fig. 24 below. The Fig. 25 can be used as a reference for typical values of static and directional stability.

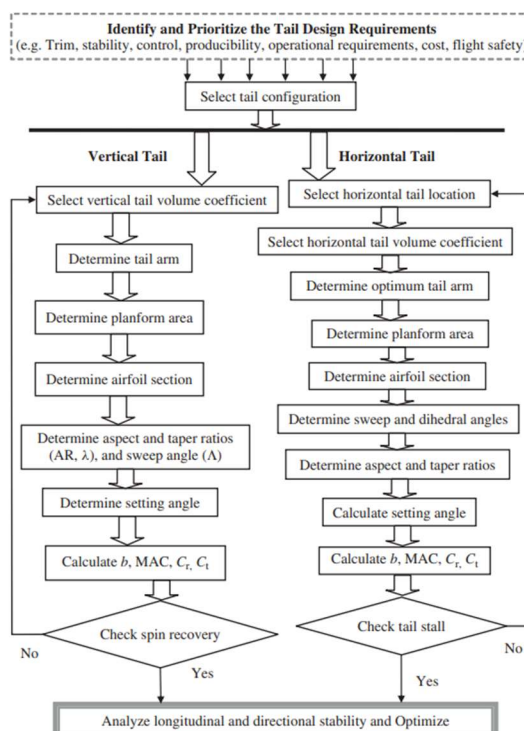


**Fig. 24 Control surface design process [27].**



**Table 6.3** The static and dynamic longitudinal and directional stability requirements

No.	Requirements	Stability derivatives	Symbol	Typical value (1/rad)
1a	Static longitudinal stability	Rate of change of pitching moment coefficient with respect to angle of attack	$C_{m\alpha}$	-0.3 to -1.5
1b	Static longitudinal stability	Static margin	$h_{np} - h_{cg}$	0.1-0.3
2	Dynamic longitudinal stability	Rate of change of pitching moment coefficient with respect to pitch rate	$C_{mq}$	-5 to -40
3	Static directional stability	Rate of change of yawing moment coefficient with respect to sideslip angle	$C_{n\beta}$	+0.05 to +0.4
4	Dynamic directional stability	Rate of change of yawing moment coefficient with respect to yaw rate	$C_{nr}$	-0.1 to -1

**Fig. 25 Typical values for static and dynamic stability of an aircraft [27].**

One of the main questions the author has struggled with while researching the tail design of SR-71 was the rotation of the *all-moving* vertical fins. The Fig. 26 below beautifully illustrates the horizontal tail setting configurations that can also be interpreted for the vertical tails. The Fig. 26 shows the fixed (a), adjustable (b), and all-moving (c) variations. The actual rotated vertical fin of the SR-71 is seen in the Fig. 27.

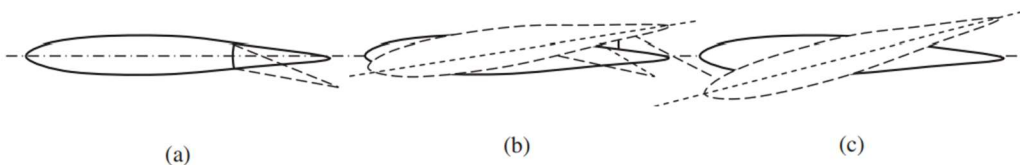


**Fig. 26 Horizontal tail setting configurations; (a) Fixed, (b) Adjustable, (c) All-moving [27].**



**Fig. 27 Vertical fin movement of the SR-71 [28].**

## 6. Roskam: Methodology search

Since the Synthesis team has chosen Roskam as their sizing methodology, Roskam could be evaluated for methods to size the vertical tail. Roskam Part II sets out an example methodology to size the vertical tail for a fighter aircraft named "Eris". This aircraft has longitudinal instability and lacks a horizontal tail. Upon reading many references, the SR-71 aircraft configuration appears to be a delta-wing with two vertical tails (tailless). Although the level of instability that's permitted for a fighter is not required for a reconnaissance aircraft, this could be a good starting point



for estimating static directional stability. Roskam also outlines methods for calculating One-Engine-Inoperative (OEI) conditions.

### 7. USAF DATCOM: Methodology search

The new reference gathered is the USAF Stability and Control DATCOM by the McDonnell Douglas corporation. This document gives extensive equations for stability in the subsonic, transonic, and supersonic regimes. The author is currently considering this reference as a potential methodology since it includes supersonic stability equations. This document gives criteria based on what kind of configuration the aircraft is with ranges for parameters like taper ratio, leading edge sweep angle, thickness-to-chord ratio, Mach number, etc.

DERIVATIVE	CONFIG.	SPEED REGIME	EQUATIONS FOR DERIVATIVE ESTIMATION (Datcom section for components indicated)	METHOD LIMITATIONS ASSOCIATED WITH EQUATION COMPONENTS
$C_{\beta}$ (Contd.)	WBT (Contd.)	SUPersonic	(Same as subsonic equation)	<ul style="list-style-type: none"> <li>1. Linear-lift range</li> <li><math>(C_{\beta})_{\text{low}}</math></li> <li>2. Straight-tapered wings</li> <li>3. Wing tips parallel to free stream</li> <li>4. Foremost Mach line from wing tip may not intersect remote half-wing</li> <li>5. <math>M &gt; 1.4</math></li> <li><math>(C_{\beta})_p</math> (based on exposed vertical-tail geometry)</li> <li>6. Additional tail limitation is identical to Item 5 immediately above</li> </ul>
$C_{n\beta}$	W	SUBSONIC (Low Speed)	$\frac{C_{n\beta}}{C_L^2} = \frac{1}{57.3} \left[ \frac{1}{4\pi A} - \frac{\tan \Lambda_{c/4}}{\pi A(A + 4 \cos \Lambda_{c/4})} \left( \cos \Lambda_{c/4} - \frac{A}{2} - \frac{A^2}{8 \cos \Lambda_{c/4}} + 6 \frac{\tilde{x}}{C} \sin \Lambda_{c/4} \right) \right]$	1. Linear-lift range
		(Subcritical)	$\left( \frac{C_{n\beta}}{C_L^2} \right)_M = \left( \frac{A + 4 \cos \Lambda_{c/4}}{AB + 4 \cos \Lambda_{c/4}} \right) \frac{(A^2 B^2 + 4AB \cos \Lambda_{c/4} - 8 \cos^2 \Lambda_{c/4})}{A^2 + 4A \cos \Lambda_{c/4} - 8 \cos^2 \Lambda_{c/4}} \left( \frac{C_{n\beta}}{C_L^2} \right)_{\text{low speed}}$	Eq. 5.1.3.1-a
	TRANSONIC	(No method)		Eq. 5.1.3.1-b
		SUPersonic	$\frac{C_{n\beta}}{\alpha^2} = \frac{1}{\pi A^2 \beta^2} \left[ \frac{4M^2}{3} + 8M^2 \frac{\tilde{x}}{C} - \pi \left[ \frac{A(1-\beta^2)}{\beta} - \frac{3+\beta^2}{3\beta^2} \right] \right] \frac{1}{57.3}$	Eq. 5.1.3.1-c
			$\frac{C_{n\beta}}{\alpha^2} = \frac{\pi}{3} \left[ \frac{E'(\theta C)}{7.1.1.1} F_9(N) + \left( \frac{A^2}{16} F_{11}(N) + \frac{\tilde{x}}{C} \right) M^2 \frac{Q(\theta C)}{5.1.1.1} \right] \frac{1}{57.3}$	Eq. 5.1.3.1-d

Fig. 28 USAF DATCOM stability equations [29].

## B. Methodologies

### 1. Static and Dynamic Stability

Stability can be further classified into two more distinct categories: static stability and dynamic stability. When a vehicle's natural tendency is to slowly return to its original position (in equilibrium) after a disturbance, we call that *static stability*. When an aircraft tends to diverge from equilibrium over time, it becomes unstable. This is an undesired effect, and usually, control power is required to trim the aircraft. When the forces and moments on an aircraft balance correctly when performing maneuvers, it is said to have *dynamic stability*. The SR-71 is said to have a slight pitch and yaw divergence, making it laterally unstable. This imposed a heavy load on the pilot to constantly control the aircraft [30]. The conceptual design often involves static stability analysis first. Dynamic stability analysis requires design data; hence it is often performed in Preliminary Design (PD) [5].

Upon reviewing methods presented in Roskam Part VII, the following steps have been determined to be taken initially. According to the text, the designer must first decide whether or not the aircraft would have Inherent Stability or De-facto stability. Inherent stability would be for an aircraft that doesn't require any form of closed-loop stability augmentation system. The de-facto stability aircraft would require such a static or dynamic augmentation system [11]. After reviewing the SR-71 flight manual for stability and control characteristics, it has become apparent that the plane had an onboard Stability-Augmentation-System (SAS) which played a critical role to manage the instability that arises from engine unstarts. Below in Fig. 29 gives a classification of SR-71 from the older regulation document MIL-F-8785C as a class III aircraft. It would mean that it is a low-to-medium maneuverability vehicle. Inverted flight is not permitted for this purpose [22].



Class	General aircraft types	Specific examples
<b>Class I</b> small, light airplanes	Light utility Primary trainer Light observation	T-41 T-6 O-1, O-2
<b>Class II</b> medium weight; low-to-medium maneuverability airplanes	Heavy utility/search and rescue Light or medium transport/cargo/tanker Early warning/ECM/Command & control Anti-submarine Assault transport Reconnaissance Tactical bomber Heavy attack Trainer for Class II	C-21 C-130 E-2 S-3A C-130 U-2 B-66 A-6 T-1A
<b>Class III</b> large, heavy, low-to-medium maneuverability airplanes	Heavy transport/cargo/tanker Heavy bomber Patrol/Early warning/ECM/Command & control Trainer for Class III	KC-10, C-17 B-52, B-1, B-2 P-3, SR-71 TC-135
<b>Class IV</b> high-maneuverability airplanes	Fighter/Interceptor Attack Tactical reconnaissance Observation Trainer for Class IV	F-22, F-15, F-16 F-15E, A-10 RF-4 OV-10 T-38

**Fig. 29 MIL-F-8785C Aircraft classes [23]**

## 2. Lateral-Directional Stability

In order to stabilize an aircraft, it is important to have a set criterion. The course textbook outlines a few of these criteria for lateral and directional stability down in Table 5. These criteria come from regulatory documents within the U.S. Column 4 in Table 5 signifies the static stability criterion. The opposite sign for the coefficients would mean that the aircraft will become unstable. The criterion for dynamic stability will be updated upon reviewing the latest MIL-HDBK-1797 military flying qualities document. The MIL-HDBK-1797 is a handbook, not the actual standard qualities listing document. The standard is called MIL-STD-1797, with 3 revisions up till 2012. This is currently a classified document; hence the handbook will be used as guidance only.

**Table 5. Lateral-Directional Stability Criteria [5].**

Symbol	Parameter	Category	Static Stabilizing	Dynamic Stabilizing	Regulations
$c_{n\beta}$	Yawing moment due to sideslip angle	Directional	> 0 (positive)		MIL-HDBK-1797
$c_{l_p}$	Roll damping derivative	Lateral	< 0 (negative)		MIL-F-8785C
$c_{l\beta}$	Rolling moment due to sideslip angle	Lateral	< 0 (negative)		MIL-HDBK-1797

Following equations from Nicolai are being considered for an initial analysis of the lateral and directional stability of a tailless aircraft [5].

$$C_{l\beta} = C_{l\beta_{wing}} + C_{l\beta_{vertical\ stabilizer}} + C_{l\beta_{wing-fuselage}} \quad (2)$$



Where  $C_{l\beta}$  is the rolling moment due to sideslip angle  $\beta$ . The terms on the right-hand side of Eq. (2) are the components influencing the derivative. Here, a negative value of  $C_{l\beta}$  will cause the aircraft to roll up from the right wing, hence laterally stabilizing it.

For directional stability, the derivative-yawing moment due to the sideslip angle  $C_{n\beta}$  is used as seen in Eq. (3) below.

$$\frac{dC_n}{d\beta} = C_{n\beta} = C_{n\beta_{fus}} + C_{n\beta_{wing}} + \bar{V}_{VT} C_{L\alpha_{VT}} \left( 1 + \frac{d\sigma}{d\beta} \right) \frac{q_{VT}}{q_\infty} \quad (3)$$

In the last term,  $\bar{V}_{VT}$  is the vertical tail volume coefficient. The coefficient  $C_{n\beta}$  must be positive for yaw stability. Usually, the rudder size must be modified to affect this derivative. A positive  $C_{n\beta}$  value is required to directionally stabilize the aircraft. Plots will have to be made for different values of  $\beta$  and their derivatives, then eventually for the coefficients. Based on the geometry, constraints charts are to be made for each criterion.

### C. Verification

Some verification methods that are being looked into are the SR-71 flight manual. The S&C team has agreed to work on producing plots as a function of angle of attack  $\alpha$  and sideslip angle  $\beta$  that show whether the aircraft is stable or not as seen in Fig. 30. Here,  $C_m$  is the pitching moment coefficient and  $C_n$  is the yawing moment coefficient.

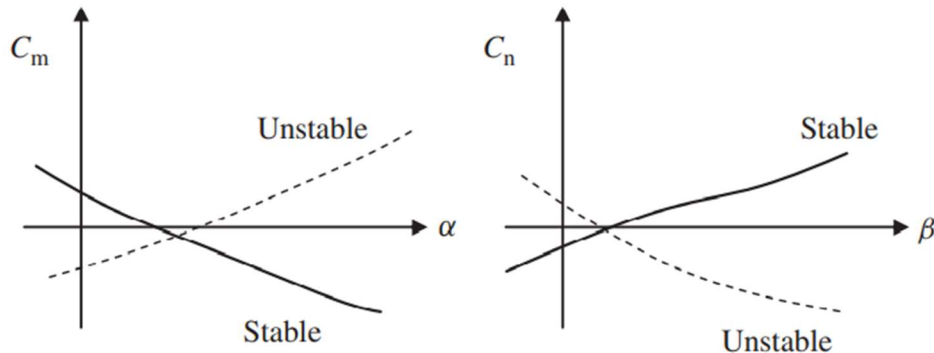


**Fig. 30 Stabilizing and de-stabilizing plots with respect to the angle of attack and sideslip [27]**

### D. Configuration Layout (CL)

For Stability and Control, the parametric sizing (PS) process is not required since the geometry, weights, and aerodynamics of the supposed aircraft need to be established, shown in the IDA (Fig. 12-14). The control surfaces to be sized for the SR-71 are twin vertical tails and inboard-outboard elevons. A list of possible aircraft configurations similar to the SR-71, in that they have a delta wing and elevons are listed below in Table 6.

**Table 6. Aircraft similar to SR-71 with delta wings and elevons.**

Symbol	Features	Inboard Elevons	Outboard Elevons
Concorde	Delta wing, 6 elevons	2	2 middle, 2 outer
Tupolev 144	Delta wing	0	8
Eurofighter Typhoon	Delta wing, elevons		2 middle 2 outer
Vulcan	Delta wing, elevons, flying wing		4 middle, 4 outer
XB-70	Delta wing, elevons	0	2 middle
B-2 Spirit Bomber	Delta flying wing, modified elevons	2	2 middle, 2 outer
F-117 Nighthawk	Delta wing, modified elevons		4 outer

### 1. Stability & Control IAO

After reviewing the course text to find equations for calculating stability derivatives, an initial IAO is drafted. This IAO will be revised after finalizing the methodology to use for convergence based on the Synthesis team's needs.

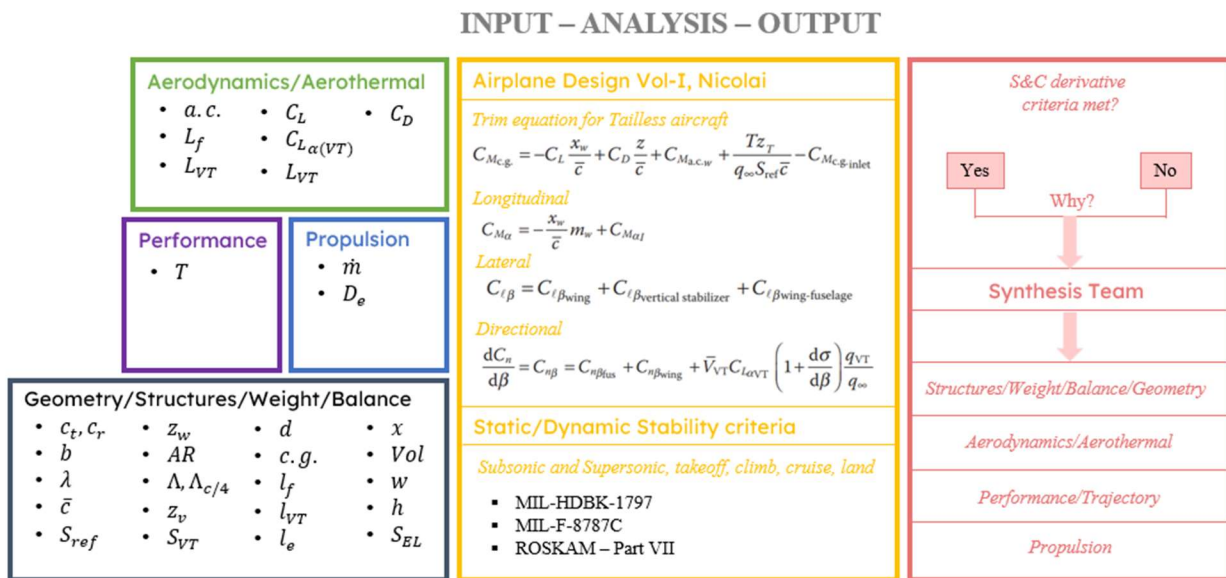


Fig. 31 Initial IAO for Stability and Control.

An IAO for stability and Control was made by the team lead, Austin. Below in Fig. 32, the IAO outlines the current plots each member is responsible for. After testing the methodology and generating the plots, this team will make an IDA that will show the chronology of the methods being used.

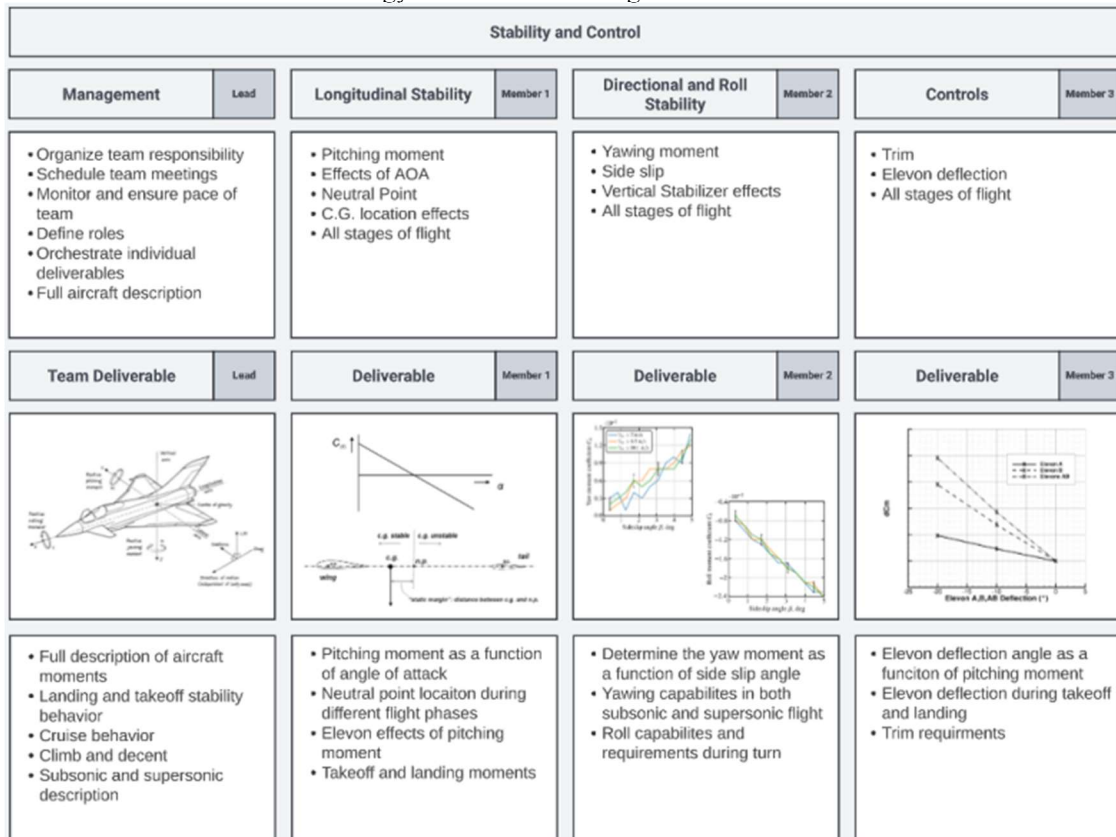


Fig. 32 Detailed IAO by the team lead Austin Prior.

 <b>PENGUIN SUPERSONIC</b>	<b>SENIOR DESIGN: MAE 4351 Project</b>	Ref.: MAE 4351-001-2021 Date: 19. Mar. 2023 Name: Gayathri Kola Status: In Progress
---	--	--

The thesis written by Stenila Simon gives a clear breakdown of conceptual design parameters necessary for each phase by PS, CL, and CE. For the Configuration Layout stage, this paper will focus on finding the applicable equations governing rolling and yawing moment coefficients,  $C_l$  and  $C_n$ . It will also detail some aspects of elevon sizing for lateral stability and vertical tail sizing for directional stability.

Categories	PS			CL			CE		
	Variable	Parameter	Units	Variable	Parameter	Units	Variable	Parameter	Units
Longitudinal	S. M.	Static Margin	m	$C_m$	Pitching moment coefficient	-	$C_{m_\alpha}$	Variation of $C_m$ coefficient with respect to AOA	-
	-	-	-	$\delta_e$	Elevator deflection angle	deg	$C_{m_q}$	Variation of $C_m$ with respect to pitch rate	-
	-	-	-	-	Elevator Area	$m^2$	-	-	-
Lateral	-	-	-	$C_l$	Rolling moment coefficient	-	$C_{l_\beta}$	Variation of $C_l$ with respect to sideslip angle	-
	-	-	-	$\delta_a$	Aileron deflection angle	deg	$C_{l_p}$	Variation of $C_l$ with respect to roll rate	-
	-	-	-	-	Aileron area	$m^2$	-	-	-
Directional	-	-	-	$C_n$	Yawing moment coefficient	-	$C_{n_\beta}$	Variation of $C_n$ with respect to sideslip angle	-
	-	-	-	$\delta_r$	Rudder deflection angle	deg	$C_{n_r}$	Variation of $C_n$ with respect to yaw rate	-
	-	-	-	-	Rudder area	$m^2$	-	-	-

Fig. 33 Parameter breakdown for each phase of Stability and Control [20].

## 2. Vertical fins sizing for directional stability

Once the PS is finished, the geometries will be used to size the control surfaces for the SR-71. The variables needed are listed in the IDA for Stability and Control (Fig 12). The methodologies being tested were from Nicolai, Raymer, and USAF Stability and Control DATCOM [5,29,31]. A reasonable range of values was taken into account to generate a plot of the rolling moment coefficient as a function of the vertical tail area (Fig. 34).

The following are the assumptions made:

- $C_{LatV} = 2\pi$  (Symmetrical airfoil for vertical tail)
- $S_{ref} = 1880.918$  ft (Appendix B)
- $AR = 1.851$  (Appendix B)
- $\Lambda_{c/4} = 58.24^\circ$  (Converted to radians, estimate provided by Noah Blakely)
- $z_v = 0$  ft (assumed)
- $d = 5.25$  ft (Estimate provided by Austin Prior based on CAD geometry)
- $z_w = 0 - 10$  ft range with 2 ft increments.
- $b = 59$  ft (Appendix B)
- $S_{vt} = 0 - 600$  ft<sup>2</sup> with 100 ft<sup>2</sup> increments

Following were the resources and equations used for the build-up:

Nicolai (Page. 591):

$$\left(1 + \frac{d\sigma}{d\beta}\right) \frac{q_{VT}}{q} = 0.724 + \frac{3.06 \left(\frac{S'_{VT}}{S_{ref}}\right)}{1 + \cos \Lambda_{c/4}} + \frac{0.4 z_v}{d} + 0.009 AR \quad (4)$$

$$(C_{l\beta})_{VT} = -C_{LatV} \left(1 + \frac{d\sigma}{d\beta}\right) \frac{q_{VT}}{q} \frac{S_{VT}}{S_{ref}} \frac{z_w}{b} \quad (5)$$

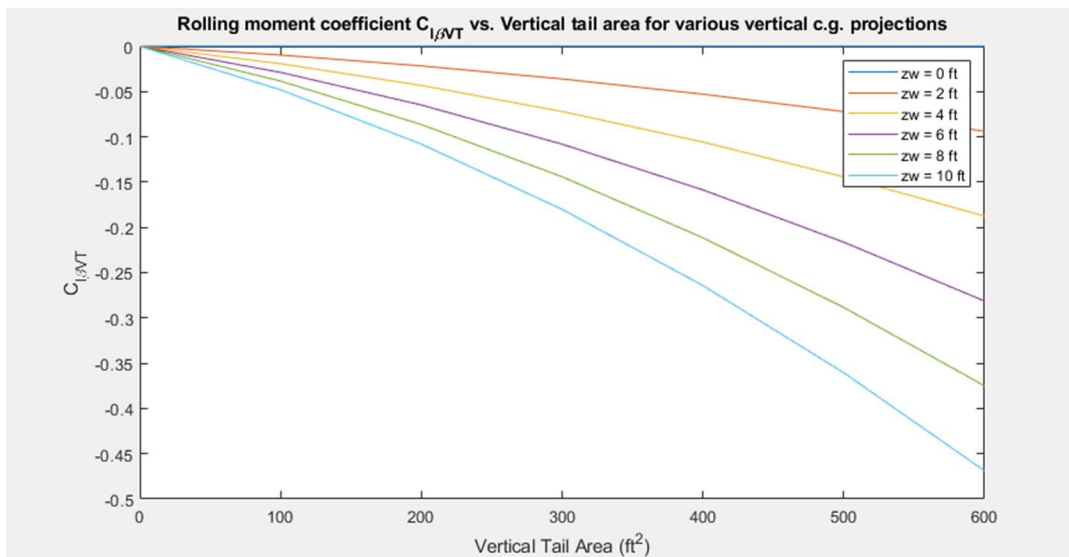


Fig. 34 Rolling moment coefficient  $C_{l\beta VT}$  vs. vertical tail area for various vertical c.g. positions.

This plot was made to see how the vertical distance from the fuselage to the vertical tail aerodynamic center would influence the vertical tail area and rolling coefficient of the vertical tail. As the area and vertical displacement increase, the more destabilizing it is for the vertical tail.

### 3. Elevons sizing for lateral stability.

The following Fig. # was produced by team member Noah for sizing the elevon area as a function of the pitching moment coefficient using the methods set out by Raymer [31]. This is the kind of analysis being aimed for lateral stability as a function of the elevon area. Currently, the right set of equations has not been found specifically for elevons. The author is looking into Raymer for further elevon analysis.

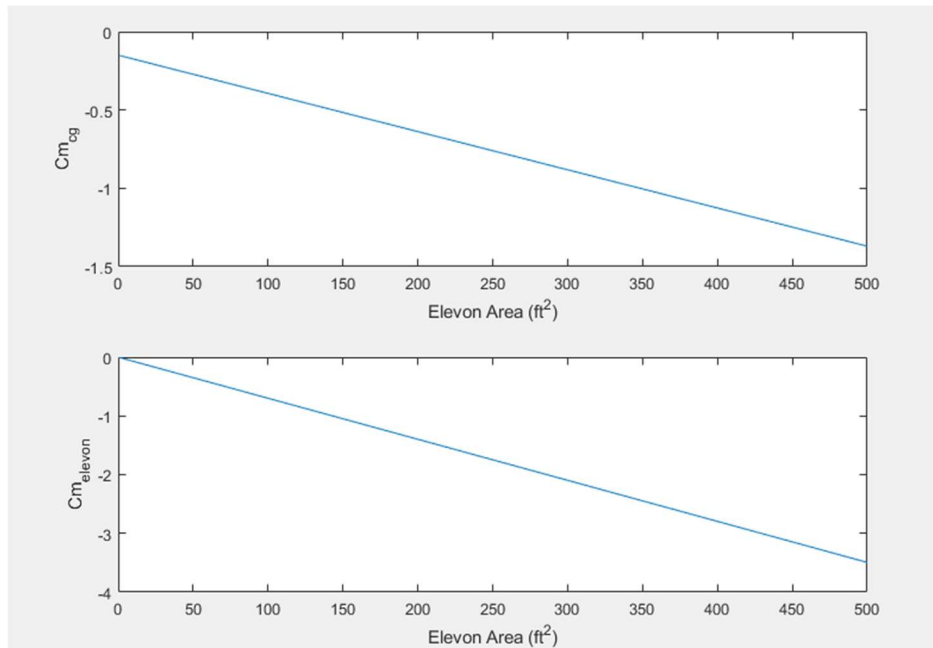


Fig. 35 Elevon sizing for pitch stability by Noah Blakely.



### E. Configuration Evaluation (CE)

For the CE phase, resources such as DATCOM and the software called OpenVSP are being considered. OpenVSP allows for a CAD model to be imported and analyzed for aerodynamics and stability and control. Specifically, analysis pertaining to trim conditions can be performed. The author is currently learning to use this software along with the CAD model provided by Austin.

Another option being considered is USAF DATCOM. There is an online coded version of the document that can be used to analyze conditions for subsonic, transonic, supersonic, and hypersonic flight based on body configuration. The following assumptions were made to produce the plot in Fig. 36:

- $\beta = 1 - 10^\circ$  (converted to radians)
- $M = 1 - 4$  (Mach number range)
- $\alpha = 1^\circ$  (angle of attack of aircraft)
- $AR = 1.851$  (Appendix B)
- $\bar{c} = 29.504$  ft (Appendix B)

Following are the equations used from DATCOM (Pages. 1-38):

$$\frac{C_{n\beta}}{\alpha^2} = \frac{1}{\pi AR^2 \beta^2} \left[ \frac{4M^2}{3} + 8M^2 \frac{x}{\bar{c}} - \pi \left\{ \frac{AR(1 - \beta^2)}{\beta} \frac{3 + \beta^2}{3\beta^2} \right\} \right] \frac{1}{57.3} \quad (6)$$

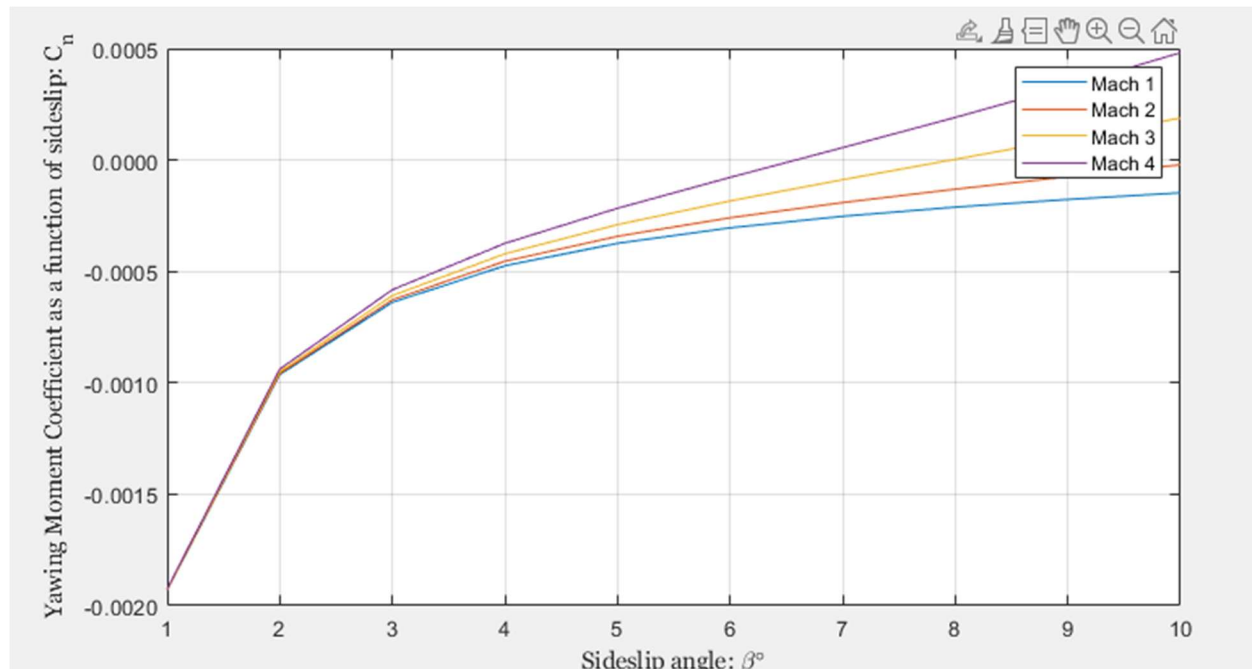


Fig. 36 Yawing moment as a function of sideslip angle for supersonic Mach numbers.

## V. Synthesis

### A. Understanding the Discipline

Before the author joined this team, the synthesis team was weighing between AVD sizing and Roskam to choose a sizing method. This week, the Synthesis team had chosen Roskam to be the appropriate sizing method. Hence, this section will go into detail about Roskam first and lay out the methodology being tested.

#### 1. Reference 1: Roskam [24]

Roskam has a simple methodology for the convergence process. It starts by first establishing the mission requirements, design trades, and a mission profile. The mission profile usually consists of phases in this order: takeoff, climb, cruise, loiter/descent, and landing. A broad search is made on similar concepts that were already made. Then,



an empirical method is used to estimate the Takeoff-Gross-Weight (TOGW) of the airplane. Roskam presents the following Eq. 4 to estimate TOGW.

$$W_{TO} = W_{OE} + W_F + W_{PL} \quad (7)$$

Where  $W_{OE}$  is the Operating Weight Empty (OWE),  $W_F$  is the fuel weight and  $W_{PL}$  is the weight of the payload. According to Roskam, there is a linear relationship between  $\log W_{TO}$  and  $\log W_E$  for supersonic cruise airplanes. The initial payload weight needs to be determined. Here, the initial payload weight is given to be 3,000 lb for the mission. Then, an initial guess is made for the takeoff weight, which is later used to determine OWE. This value of OWE is plugged back into Eq. 4 to obtain a new value of TOGW. This TOGW is then iterated until there is a converged solution. The Fig. 37 below illustrates the empirical method used for estimating  $W_{OE}$ . Once the TOGW is estimated, a set of constraints are selected for analysis, namely stall, landing distance, takeoff field length, climb gradient, cruise conditions, and maneuvering flight. These constraints are calculated as a function of the wing loading (W/S) and/or thrust loading (T/W). A performance matching diagram is generated with all the constraint plots from which the solution space can be visualized as seen in Fig. 38. The match point is chosen for minimum thrust loading (T/W) to get an estimate of the maximum TOGW needed.

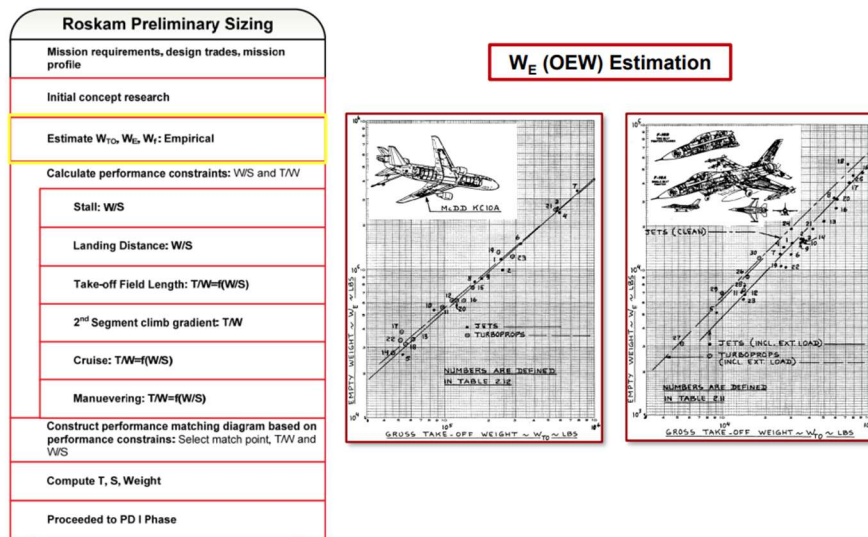


Fig. 37 Roskam Preliminary Sizing process and Operating Empty Weight estimation [8]

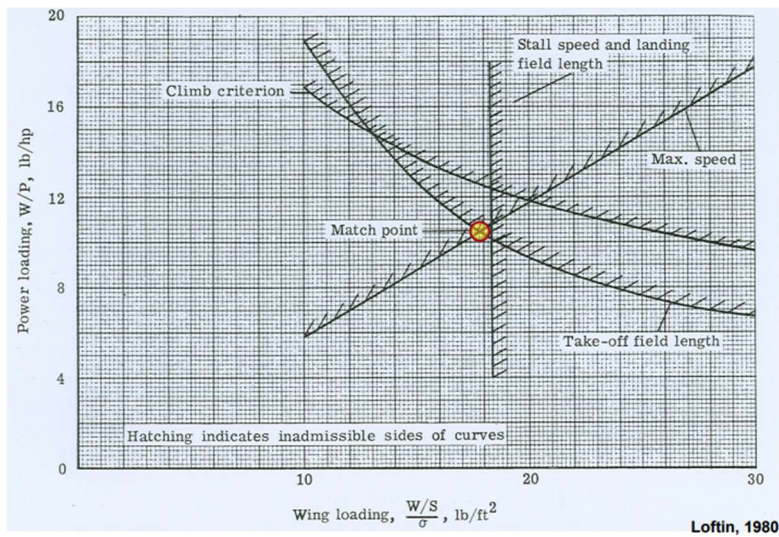


Fig. 38 An example of a matching point diagram to generate a solution space [6].

 <b>PENGUIN SUPERSONIC</b>	<b>SENIOR DESIGN:</b> <b>MAE 4351 Project</b>	Ref.: MAE 4351-001-2021 Date: 19. Mar. 2023 Name: Gayathri Kola Status: In Progress
---	--	--

Once the design match point is chosen, the W/S and T/W are chosen for a TOGW. The new OEW is calculated as a function of TOGW. A new estimate was made for TOGW based on payload weight, fuel weight, and the value of OEW. The convergence will happen when the difference between old TOGW and new TOGW is less than or equal to a specified tolerance. The convergence process for Roskam sizing is long and difficult since a single change in a parameter requires the whole process to be restarted again.

$$|TOGW_{old} - TOGW_{new}| \leq tolerance \quad (8)$$

## 2. Reference 2: Hypersonic Convergence

Another method named Hypersonic Convergence was developed by Paul A. Czysz back in 1980. Traditionally, the sizing logic involves first sizing the wing and propulsion system first and later adding fuselage and empennage sizing using empirical methods laid out in methods such as Roskam. However, hypersonic convergence combines the volume of the body into its convergence process. This is done by utilizing two core equations solving for the weight (OEW) and volume (OWE) budget equations given in Eq. (12-14). This method introduces a new variable called the slenderness ratio  $\tau$ . This equates the volume of the vehicle to its planform area. This ratio can be used to estimate how slender an aircraft body is. The higher the value of  $\tau$ , the larger the vehicle is.

$$\tau = \frac{Vol}{S_{pln}^{1.5}} \quad (9)$$

The following Fig. 39 shows the difference in the process for hypersonic convergence and traditional sizing logic. First, a geometry is chosen from a family of configurations outlined by Paul. A. Czysz as seen in Fig. 43. The propulsion system is chosen along with the gross configuration, and other necessary constraints are defined. For the iteration process, first, the geometry is developed based on the chosen slenderness ratio  $\tau$ . The wetted area per planform area  $k_w$  is computed to use in the weight budget equation (Eq. 12). This is different from the classical sizing logic where the thrust loading and wing loading are both iterated to estimate OEW. This would result in a large amount of data to process. For trajectory analysis, the total weight ratio (WR) is obtained by performing calculations for fuel fractions for segments of the flight trajectory. This is an independent analysis that can be performed using methods set out by Roskam, and Loftin, depending on mission requirements and speed regime.

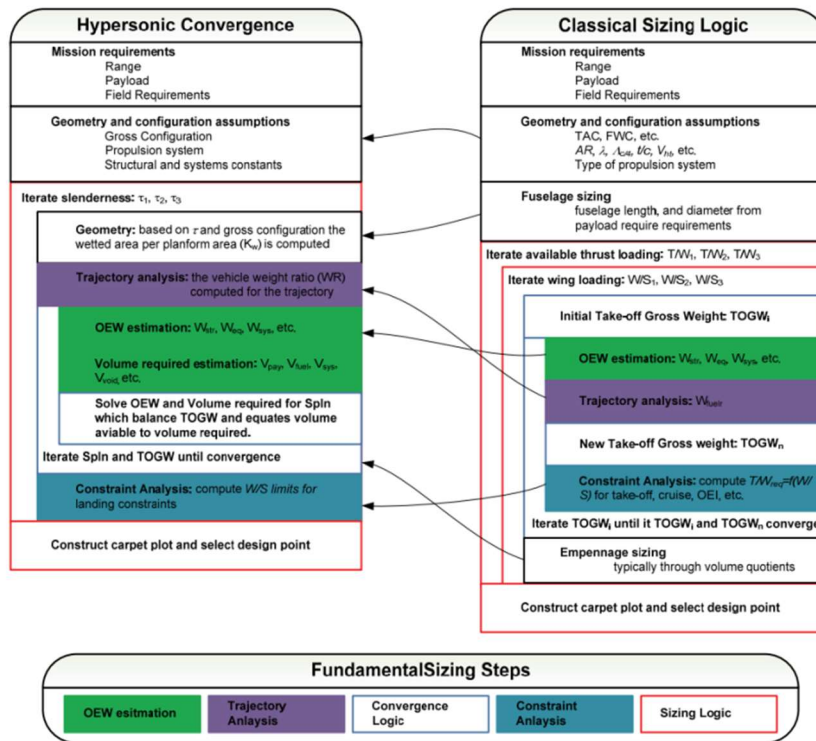


Fig. 39 Difference between Hypersonic Convergence and classical sizing logic [8].



The whole process is iterated for a range of slenderness ratios depending on chosen geometry. Each value of  $\tau$  has a specific wing loading associated with it. The map of converged design points is produced for each value of  $\tau$ . Then, the landing constraint analysis is performed such as approach speed for maximum wing loading. For a given planform area, the minimum TOGW is used as the main design point (seen in Fig. 40) and a carpet plot is made showing the solution space.

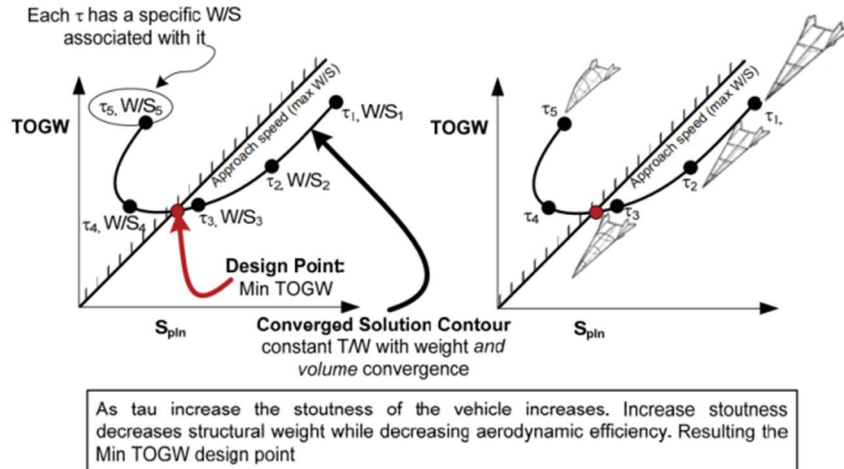


Fig. 40 Hypersonic convergence design point estimation [8].

### 3. Reference 3: AVD Sizing

This method is similar to hypersonic convergence, but it combines the constraint analysis within the convergence logic. This allows for varying a specific independent design parameter such as aspect ratio, taper ratio, leading-edge sweep, or critical Mach number before iterating for  $\tau$ . The slenderness ratio is held constant and the geometry, trajectory, and constraint analysis is performed. The weight and volume budget equations are computed independently, with the planform area being iterated until they converge.

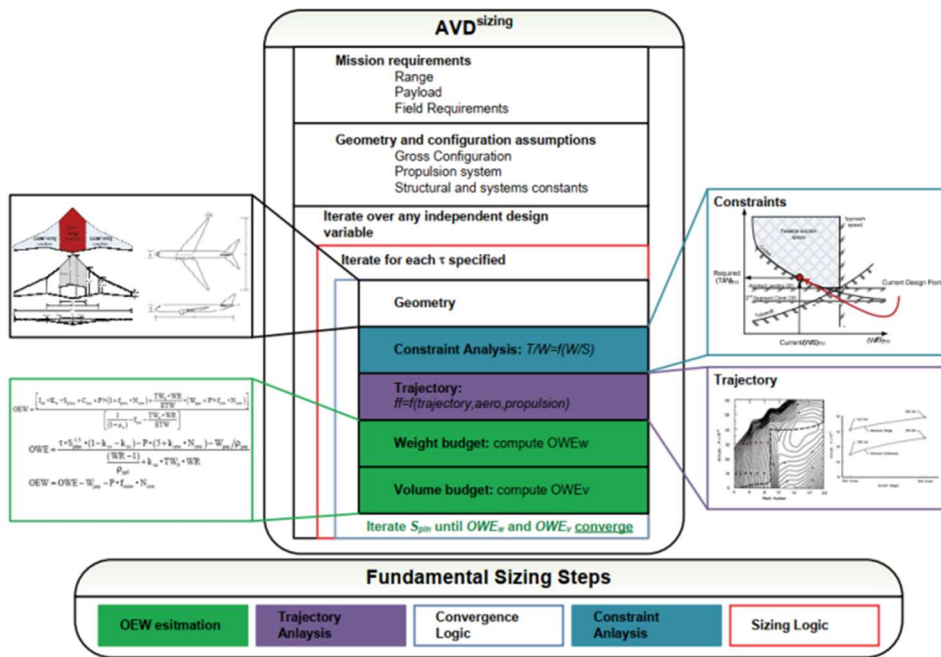


Fig. 41 AVD sizing logic [8].



## B. Parametric Sizing (PS)

The Synthesis team has elected to use Hypersonic convergence for the sizing methodology. This methodology was chosen since it is the best way to size the aircraft quickly and reliably. The mission profile was updated after discussing with competing teams to add an accelerated climb segment after takeoff. The PS stage involves constraints analysis where the performance is calculated as a function of W/S (wing loading) and T/W (thrust loading).

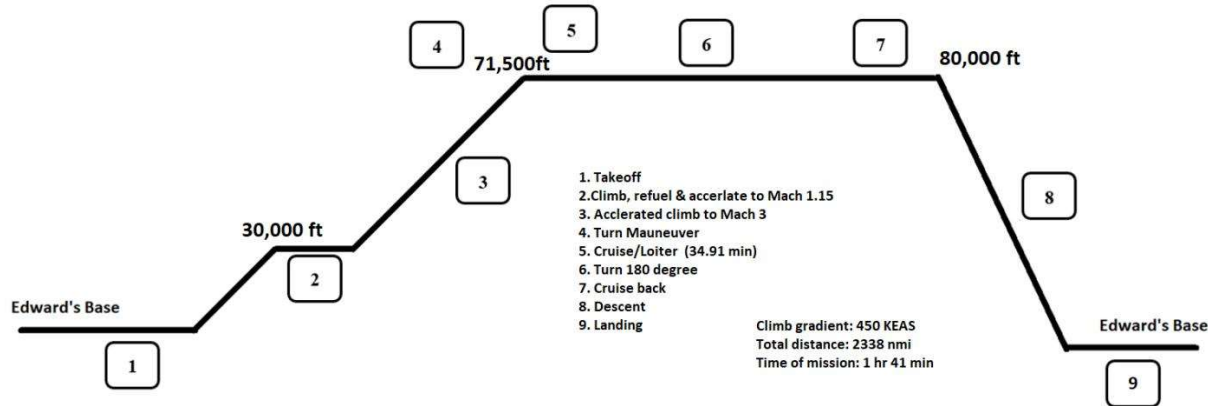


Fig. 42 The SR-71 mission profile created by Phat Nguyen.

### 1. Segregating tasks among disciplines

For convergence, the variables in the OWE and OEW equations are identified and segregated among disciplines. The variable names and ranges are given in the Fig. 48. Each discipline must conduct its independent analysis of the required variables to provide a range of suitable values to the Synthesis team. The Synthesis team will use these values by iterating the slenderness ratio to obtain values of TOGW and  $S_{pln}$ . A solution space will be obtained for a chosen configuration (examples given in Fig. 40).

### 2. Estimating Slenderness Ratio ( $\tau$ )

An initial TOGW guess was taken to be 140,000 lb based on the previous Roskam sizing method. The slenderness ratio can be estimated based on various families of geometries given in the Hypersonic Convergence methodology by Paul A. Czysz. The Fig. 43 below shows the slenderness ratio as a function of the ratio between the wetted area and planform area  $k_w$  for multiple geometric configurations.

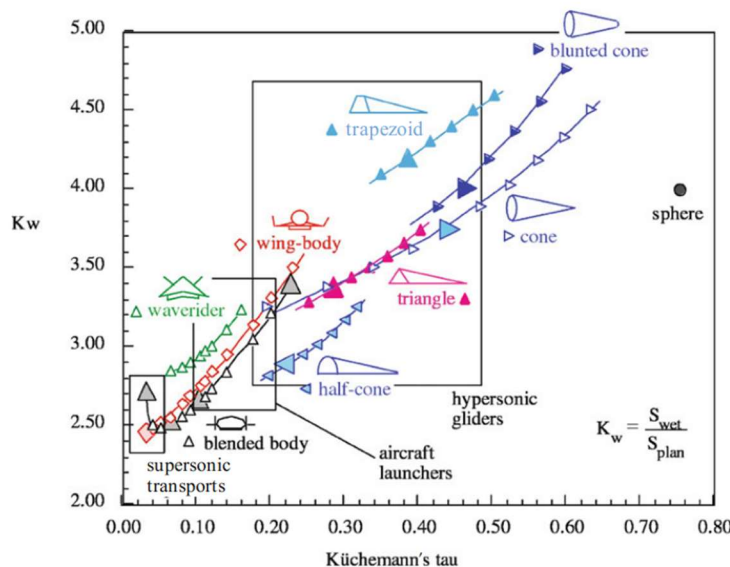
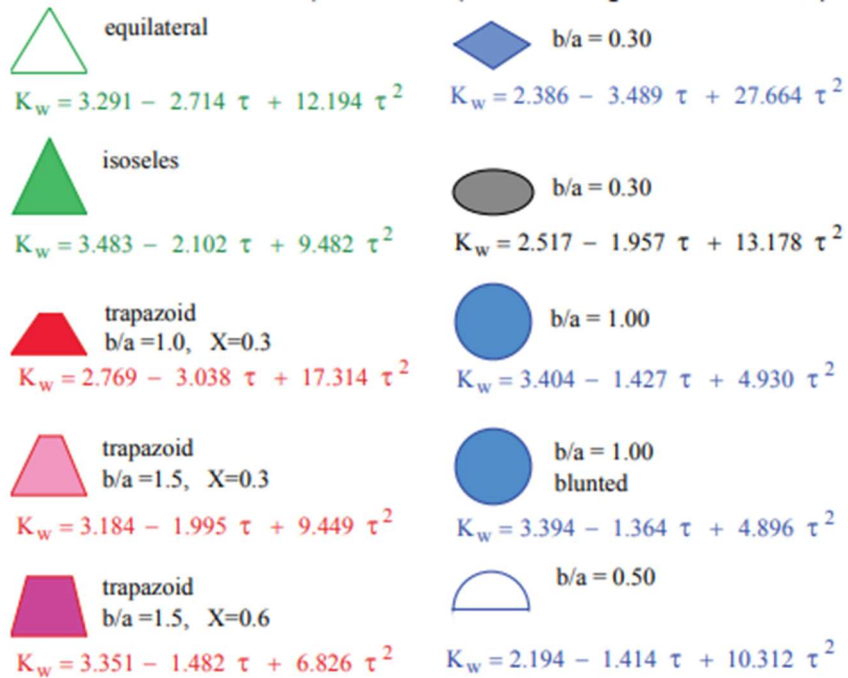


Fig. 43 The  $k_w$  as a function of slenderness ratio for various geometries [19].

 <b>PENGUIN SUPERSONIC</b>	<b>SENIOR DESIGN: MAE 4351 Project</b>	Ref.: MAE 4351-001-2021 Date: 19. Mar. 2023 Name: <b>Gayathri Kola</b> Status: In Progress
---	--	---



**Fig. 44 Relationship between slenderness ratio and  $k_w$  [8].**

The Geometry team member, Austin, has produced an analysis of slenderness ratio ( $\tau$ ) for various configurations along with an estimated value of  $\tau$  based on his CAD model of the SR-71. The Fig. 45 below shows  $k_w$  as a function of  $\tau$  for various configurations. This is very helpful for having a starting guess of the  $\tau$  range to be iterated for sizing. Currently, the diamond, half-diamond, and elliptical appear to be the closest to the estimated SR-71 value. The  $\tau$  range chosen for initial sizing will be from 0 to 0.06. This appears to be falling in the supersonic range as seen in Fig. 43.

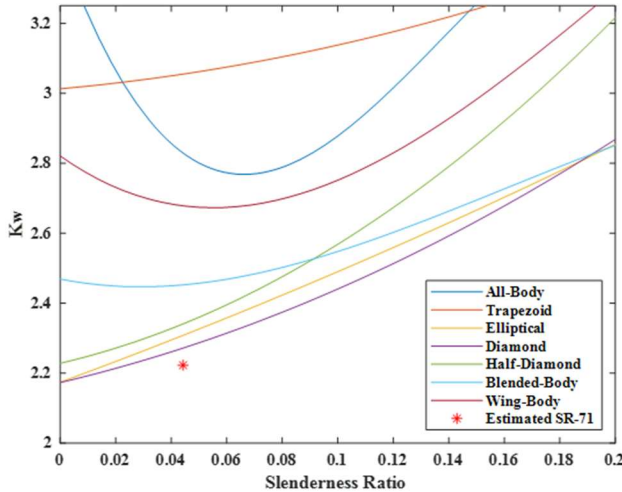


**Fig. 45 The  $k_w$  as a function of slenderness ratio for various configurations by Austin Prior.**

### 3. Trajectory Analysis

The Performance team is tasked with conducting a trajectory analysis based on the chosen mission profile and providing the Synthesis team with the overall Weight-Ratio (WR) for the mission. The performance team is using Roskam as the methodology for performing this analysis. The overall WR will be calculated using the overall fuel fraction using Eq. (10) below.

 <b>PENGUIN SUPERSONIC</b>	SENIOR DESIGN: MAE 4351 Project	Ref.: MAE 4351-001-2021 Date: 19. Mar. 2023 Name: Gayathri Kola Status: In Progress
---	------------------------------------	--

$$WR = \frac{1}{1 - ff} \quad (10)$$

First, the takeoff weight is estimated using Eq. 4. Eq. 5 below is used to estimate OWE.

$$W_{OE} = W_E + W_{tfo} + W_{crew} \quad (11)$$

Where  $W_E$  is the empty weight,  $W_{tfo}$  is the trapped fuel and oil, and  $W_{crew}$  is the weight of the crew. The fuel weight  $W_F$  is estimated using the fuel-fraction method outlined in Roskam. A MATLAB code was made by the chief engineer Wesley to estimate the overall fuel fraction based on methods given in Roskam. The Fig. 46 below can be used to estimate fuel fractions for a supersonic cruise based on mission phases. The numbers associated with each flight phase can be used to calculate the beginning and end weights.

**Table 2.1 Suggested Fuel-Fractions For Several Mission Phases**

Mission Phase No. (See Fig. 2.1)	1	2	3	4	7	8	Landing Taxi, Shutdown
Airplane Type:							
1. Homebuilt	0.998	0.998	0.998	0.995	0.995	0.995	0.995
2. Single Engine	0.995	0.997	0.998	0.992	0.993	0.993	0.993
3. Twin Engine	0.992	0.996	0.996	0.990	0.992	0.992	0.992
4. Agricultural	0.996	0.995	0.996	0.998	0.999	0.998	0.998
5. Business Jets	0.990	0.995	0.995	0.980	0.990	0.990	0.992
6. Regional TBP's	0.990	0.995	0.995	0.985	0.985	0.995	0.995
7. Transport Jets	0.990	0.990	0.995	0.980	0.990	0.992	0.992
8. Military Trainers	0.990	0.990	0.990	0.980	0.990	0.995	0.995
9. Fighters	0.990	0.990	0.990	0.96-0.90	0.990	0.990	0.995
10. Mil. Patrol, Bomb, Transport	0.990	0.990	0.995	0.980	0.990	0.990	0.992
11. Flying Boats, Amphibious, Float Airplanes	0.992	0.990	0.996	0.985	0.990	0.990	0.990
12. Supersonic Cruise	0.990	0.995	0.995	0.92-0.87	0.985	0.992	0.992

Fig. 46 Fuel fractions for different types of aircraft at various mission phases [24].

#### 4. Weight and Volume budgets

The weight and volume budget equations, OEW and OWE are solved for the planform area for a specific TOGW. The following are the weight  $W_{OEW}$  and volume  $W_{OWE}$  budget equations used in the convergence process. The variables are color-coded to indicate the category associated with them.

$$W_{OEW} = \frac{I_{str} k_w S_{pln} + C_{sys} + \frac{\left(\frac{T}{W}\right)_{MAX} W_R}{E_{TW}} (W_{pay} + W_{crew}) + W_{cpnv}}{\frac{1}{1 + \mu_a} - f_{sys} - \frac{\left(\frac{T}{W}\right)_{MAX} W_R}{E_{TW}}} \quad (12)$$

$$W_{OWE} = \frac{I_{str} S_{pln}^{1.5} (1 - k_{vv} - k_{vs}) - v_{fix} - N_{crw} (v_{crw} + k_{crw}) - \frac{W_{pay}}{\rho_{pay}}}{\frac{W_R - 1}{\rho_{ppl}} + \left( k_{ve} \left( \frac{T}{W} \right)_{MAX} W_R \right)} \quad (13)$$

$$W_{OWE} = W_{OEW} + W_{pay} + W_{crew} \quad (14)$$

The variable  $I_{str}$  is the structural index, the ratio between structural weight  $W_{str}$  and wetted area  $S_{wet}$  of the aircraft. The structural weight can be calculated using the following equation below:



$$W_{str} = k_{str} * S_{pln}^{1.38*OEW} \quad (15)$$

The list of variables and their relations to hypersonic convergence are given in Fig. 47. The coefficients with no relationship such as the fuel density, payload density, etc, are estimated based on the type of vehicle.

Table 4-1: Weight and Volume Budget Terms from Hypersonic Convergence <sup>(64)</sup>

Variable	Description	Hypersonic Convergence Relationship
<b>Weight Budget</b>		
$W_{str}$	Structural weight	$W_{str} = I_{str} S_{wet}$
$W_{sys}$	Systems weight	$W_{sys} = C_{sys} + f_{sys} W_{OEW}$
$W_{eng}$	Engine weight	$W_{eng} = \frac{T / W \cdot WR}{E_{TW}} OWE$
$C_{sys}$	Constant systems weight	-
$f_{sys}$	Variable systems weight	-
$E_{TW}$	Engine thrust to weight ratio	
$I_{str}$	Structural index	See methods library
<b>Volume Budget</b>		
$V_{fuel}$	Fuel volume	$V_{fuel} = \frac{OWE \cdot (WR - 1)}{\rho_{fuel}}$
$V_{fix}$	Fixed system volume	$V_{fix} = V_{un} + V_{optems}$
$V_{sys}$	Total system volume	$V_{sys} = V_{fix} + k_{vs} V_{tot}$
$V_{eng}$	Engine volume	$V_{eng} = k_{ve} \cdot T / W \cdot WR \cdot OWE$
$V_{void}$	Void volume	$V_{void} = k_{vv} V_{tot}$
$V_{pay}$	Payload volume	$V_{pay} = W_{pay} / \rho_{pay}$
$V_{crw}$	Crew volume	$V_{crw} = k_{crw} N_{crw}$
$V_{tot}$	Total volume	$V_{tot} = \tau \cdot S_{pln}^{1.5}$
$V_{un}$	Unused volume	-
$V_{optems}$	Operational items volume	-
$\rho_{fuel}$	Fuel density	-
$\rho_{pay}$	Payload density	-
$k_{ve}$	Engine volume coefficient	-
$k_{vv}$	Void volume coefficient	-
$k_{vs}$	Variable systems volume	-

Fig. 47 Hypersonic Convergence variables and the relationships [25]

For an initial estimate of the values, Fig. 48 helped obtain some of the ranges.

 <b>PENGUIN SUPersonic</b>	SENIOR DESIGN: MAE 4351 Project	Ref.: MAE 4351-001-2021 Date: 19. Mar. 2023 Name: <b>Gayathri Kola</b> Status: In Progress
---	------------------------------------	---

$W_{\text{str}} = I_{\text{str}} \cdot K_w \cdot S_{\text{pln}} + W_{\text{cpv}}$	$17 \leq I_{\text{str}} \leq 23 \text{ kg/m}^2$
$W_{\text{sys}} = C_{\text{sys}} + f_{\text{sys}} \cdot W_{\text{dry}}$	$0.16 \leq f_{\text{sys}} \leq 0.24 \text{ ton/ton}$
$C_{\text{sys}} = C_{\text{un}} + f_{\text{mnd}} \cdot N_{\text{crw}}$	$1.9 \leq C_{\text{un}} \leq 2.1 \text{ ton}$
	$1.45 \leq f_{\text{mnd}} \leq 1.05 \text{ ton/person}$
$W_{\text{eng}} = \frac{TW_0 \cdot W_R}{E_{\text{TW}}} \cdot (W_{\text{dry}} + W_{\text{pay}} + W_{\text{crw}})$	$10 \leq E_{\text{TW}} \leq 25 \text{ kg thrust/kg weight}$
$W_{\text{cpv}} = f_{\text{cpv}} \cdot N_{\text{crw}}$	$0.45 \leq f_{\text{cpv}} \leq 0.50 \text{ ton/person}$
$W_{\text{crw}} \cdot N_{\text{crw}}$	$0.14 \leq f_{\text{crw}} \leq 0.15 \text{ ton/person}$
$V_{\text{tot}} = \tau \cdot S_{\text{pln}}^{1.5}$	$0.032 \leq \tau \leq 0.20$
$V_{\text{ppl}} = W_{\text{OE}} \cdot \frac{(WR - 1)}{\rho_{\text{ppl}}}$	$5.0 \leq V_{\text{un}} \leq 7.0 \text{ m}^3$
$V_{\text{fix}} = V_{\text{un}} + f_{\text{crw}} \cdot N_{\text{crw}}$	$11.0 \leq f_{\text{crw}} \leq 12 \text{ m}^3 / \text{person}$
$V_{\text{sys}} = V_{\text{fix}} + K_{\text{vs}} \cdot V_{\text{tot}}$	$0.02 \leq k_{\text{vs}} \leq 0.04 \text{ m}^3/\text{m}^3$
$V_{\text{eng}} = k_{\text{ve}} \cdot TW_0 \cdot W_R \cdot W_{\text{OE}}$	$0.25 \leq k_{\text{ve}} \leq 0.75 \text{ m}^3/\text{ton thrust}$
$V_{\text{void}} = k_{\nu\nu} \cdot V_{\text{tot}}$	$0.10 \leq k_{\nu\nu} \leq 0.20 \text{ m}^3/\text{m}^3$
$V_{\text{pay}} = W_{\text{pay}}/\rho_{\text{pay}}$	$48 \leq \rho_{\text{pay}} \leq 130 \text{ kg/m}^3$
$V_{\text{crw}} = (V_{\text{pcrv}} + k_{\text{crw}}) \cdot N_{\text{crw}}$	$0.9 \leq k_{\text{crw}} \leq 2.0 \text{ m}^3/\text{person}$
	$6.0 \leq V_{\text{pcrv}} \leq 5.0 \text{ m}^3/\text{person}$

**Fig. 48 Coefficient ranges for Weight and Volume Budget equations [32].**

A baseline code was developed using the lowest values in the coefficient ranges with no iterations.

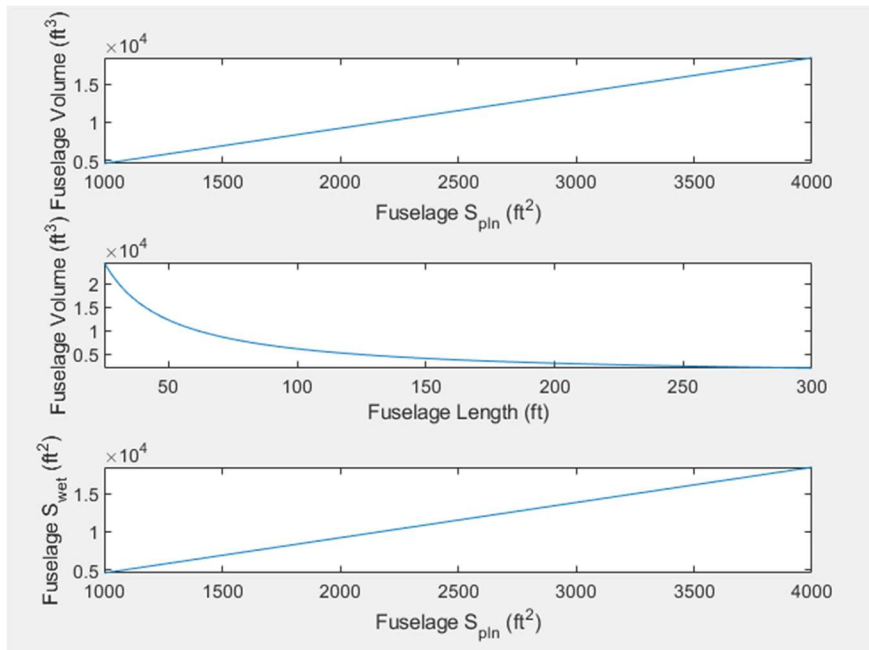


**Fig. 49 Geometry change based on solution space geometry by Austin Prior.**

### C. Configuration Layout (CL)

## VI. Conclusion

## Appendix

### A. Costs and Market Estimates Appendix

**Table 7. Literature Review for Costs and Market Estimates.**

Serial No.	Title	Author	Year	Category
1	Airplane Design Part VIII: Cost Estimation: Design, Development, Manufacturing, and Operating [33]	Jan Roskam	2015	Book
2	US Military Aircraft Cost Handbook [34]	DePuy, W. E. Moyer, R.	1983	Book
3	The Minimization of Combat Aircraft Life-Cycle-Cost through Conceptual Design Optimization [35]	Woodford, S.	1999	Thesis
4	Statistical-Analytical Model for Cost Estimation and Economic Optimization of Launch Vehicles [36]	Koelle, D. E.	2013	Book
5	The Lockheed SR-71 Blackbird – A Senior Design Capstone Re-Engineering Experience [13]	Mixon, B. Chudoba, B.	2007	Article
6	DAPCA: A Computer Program for Determining Aircraft Development and Production Costs [37]	Boren, H. E.	1967	Book
7	Fundamentals of Aircraft and Airship Design Volume II – Airship Design & Trade Studies [38]	Carichner, G Nicolai, L. M	2013	Book
8	An Estimation of USAF Aircraft Operating and Support Cost Relations [39]	Hildebrandt, G. Sze, M.	1990	Report
9	Aircraft Airframe Cost Estimating Relationships Study Approach and Conclusions [40]	Hess, R. Romanoff, H.	1987	Book
10	Commercial Airplane Design Principles [41]	Sforza, P. M.	2014	Book

 <b>PENGUIN SUPERSONIC</b>	<b>SENIOR DESIGN: MAE 4351 Project</b>	Ref.: MAE 4351-001-2021 Date: 19. Mar. 2023 Name: <b>Gayathri Kola</b> Status: In Progress
---	--	---

Inputs	
Propulsion	<ul style="list-style-type: none"> <li>Mission Fuel, oil, lubricants (lbs)</li> <li>Fuel density (lbs per U.S. gallon)</li> </ul>
Performance & Trajectory	<ul style="list-style-type: none"> <li>Mission Profile: Single, Multi-legged</li> <li>Mission Profile time, per leg</li> </ul>
Structures/Weight/Balance/Geometry	<ul style="list-style-type: none"> <li>Total area (in sqft) of all access panels in the airplane</li> <li>Empty weight, TOGW, Maximum velocity (kts)</li> </ul>
Analysis	
ROSKAM - Part VIII	
Life-Cycle-Costs (LCC)	
C(RDTE): Research, Development, Test, and Evaluation	C(POLS): Program Fuel cost
C(ACQ): Program Acquisition Cost	C(PERDIR): Direct Personnel
C(OPS): Program Operating Cost	C(PERSIND): Indirect Personnel
C(DISP): Program Disposal Cost	C(CONMAT): Consumable Materials Cost
C(UNIT): Aircraft Unit Cost	C(SPARES): Spares Costs
Design Optimization	C(DEPOT): Depot Costs
Design-To-Cost	C(MISC): Miscellaneous Costs
Outputs	
SYNTHESIS TEAM	<ul style="list-style-type: none"> <li>Life Cycle Cost (LCC)</li> <li>Operations Costs</li> <li>Unit Costs</li> <li>Market feasible?</li> </ul> 

**Fig. 50 Initial IAO for Costs and Market Estimates.**

## B. Stability and Control Appendix

Lateral-directional coefficients as a function of sideslip angle codes.

```
% STABILITY AND CONTROL: DIRECTIONAL STABILITY
% CONFIGURATION: Wing

% INPUTS:

% _____Geometry_____
% l      - length of fuselage [ft]
% lf     - distance from c.g to fuselage sideforce [ft]
% lvt    - distance from c.g to vertical tail c.g [ft]
% Sref   - wing reference area [ft^2]
% Svt    - vertical tail area [ft^2]
% b      - span [ft]
% Nwing  - Wing moment [lb-ft]
% zw    - distance along aircraft z axis from the wing root chord to the fuselage centerline [ft]
% d      - max fuselage depth [ft]

% _____Aerodynamics_____
% CL     - Lift coefficient [-]
% AR     - Aspect Ratio [-]
```



```
% Sweep      - Leading Edge Sweep [deg]
% SweepC4    - Sweep at quarter chord [deg]
% Cbar       - mean aero chord [ft]
% CLavt      - lift-curve-slope of vertical tail [-]

% _____Propulsion_____
% Npower     - Engine Moment [lb-ft]

% _____Weights_____
% xcg        - center of gravity of aircraft [ft]
% xcgVT      - center of gravity of vertical tail [ft]

% q          - dynamic pressure
% qvt        - dynamic pressure on vertical tail
% mach       - mach number [-]
% alt        - altitude [ft]
% ---

clc
clear all

% GEOMETRY
xcg = input('Aircraft C.G. location [ft]: ');
Sideforce = input('Sideforce location on fuselage from fuselage start line in %: ');
Tailac = input('Tail a.c. locaiton from fuselage start line in %: ');
l = 105.373;
lf = xcg - (Sideforce*l);
lvt = (Tailac*l) - xcg;
Sref = 1880.918;
Svt = 106.593;
b = 59;
Vol = 1325.71;
h = 5.42;
w = 12;
Wingac = input('Wing a.c [ft]: ');
x = xcg - Wingac;

% AERODYNAMICS
CL = 0.9;
AR = 1.851;
Sweep = 60;
SweepC4 = 58.24;
Cbar = 29.504;
CLavt = 2*pi; % Symmetric tail airfoil

% PROPULSION
Npower = 0;
Nwing = 0;
% ---

% OTHER
xcg = 0.55*l;
xcgVT = 0.78*l;
zw = 0; %[ft]
d1 = 1; %[ft]

LF = input('Sideforce on the fuselage [lb]: '); %[lb]
alt = input('Altitude [ft]: '); %[ft]
Mach = input('Mach number [-]: ');
[Temp,Press,rho,SOS] = FeetStandardAtmosphere(alt);
velocity = Mach * SOS;
q = 0.5 * rho * velocity^2;
% ---

beta = 1:1:15;
CN = zeros(length(beta),1);
```

 <b>PENGUIN SUPERSONIC</b>	<b>SENIOR DESIGN:</b> <b>MAE 4351 Project</b>	Ref.: MAE 4351-001-2021 Date: 19. Mar. 2023 Name: <b>Gayathri Kola</b> Status: In Progress
---	--	---

```

for i = 1:length(beta)
    CN(i,1) = Cn(1f,LF,lvt,Svt,b,Sref,CLavt,SweepC4,zw,d1,AR,Npower,Nwing,q,beta(i));
end

SweepC4i = [30:5:70] * (pi/180);
CNBeta = zeros(length(SweepC4i),1);

for j = 1:length(SweepC4i)
    CNBeta(j,1) = CnBeta(Vol,Sref,b,h,w,CL,AR,SweepC4(j),Cbar,x,lvt,Svt,CLavt,zw,d1);
end

figure(1)
plot(beta(:,1),CN(:,1))
xlabel('Sideslip angle: \beta\circ');
ylabel('Yawing moment coefficient: C_n');

figure(2)
plot(SweepC4i,CNBeta(:,1))
xlabel('Sideslip angle: \beta\circ');
ylabel('Yawing moment coefficient: C_n');

% Function file: (1)-----
function Cn = Cn(1f,LF,lvt,Svt,b,Sref,CLavt,SweepC4,zw,d,AR,Npower,Nwing,q,beta)

    % SweepC4 >> radians
    % beta >> radians

    % NICOLAI 21.15: Downwash term - (1+dsdbeta)*(qvt/q)
    K1 = 0.724 + ( (3.06 * (Svt/Sref))/(1+cos(SweepC4)) ) + (0.4*(zw/d)) + (0.009*AR);

    % NICOLAI: BetaVT - (1+dsdbeta)*beta
    betaVT = K1 * beta;

    % NICOLAI 21.19: Cn
    Cn = -(1f*LF/(q*Sref*b)) + ((lvt*Svt/b*Sref)*Clavt*betaVT) + (Npower/(q*Sref*b)) + (Nwing/(q*Sref*b));
end

%% Function file: (2)-----
function CNBeta = CnBeta(Vol,Sref,b,h,w,CL,AR,SweepC4,Cbar,x,lvt,Svt,CLavt,zw,d)

    % SweepC4 >> radians

    % NICOLAI 21.15: Downwash term - (1+dsdbeta)*(qvt/q)
    K1 = 0.724 + ( (3.06 * (Svt/Sref))/(1+cos(SweepC4)) ) + (0.4*(zw/d)) + (0.009*AR);

    % NICOLAI 21.23: Cn fuselage
    CnFuselage = -1.3 * (Vol/(Sref*b)) * (h/w);

    % NICOLAI 21.22: Cn wing
    CnWing = CL^2 * ( (1/4*pi*AR) - (tan(SweepC4) / (pi*AR*(AR+(4*cos(SweepC4)))) * (cos(SweepC4) - (AR/2) - (AR^2/(8*cos(SweepC4))) * ((6*x*Cbar)*(sin(SweepC4)/AR))) );

    % NICOLAI: Vertical tail coefficient Vvt
    Vvt = (lvt*Svt/(b*Sref));

    % NICOLAI 21.21: CnBeta Vertical tail
    CnBetaVT = Vvt * Clavt * K1;

    % NICOLAI 21.20: Directional stability derivative
    CNBeta = CnFuselage + CnWing + CnBetaVT;
end

```



Code segment for  $C_{n\beta}$  as a function of sideslip angle and Mach number:

```
M = 1:1:4;
beta2 = [1:1:10] .* (pi/180);
alpha = 1 * (pi/180);
for j = 1:length(M)
    for k = 1:length(beta2)
        CnBeta(k,j) = alpha^2 * (1/pi*AR^2*beta2(k)^2)*(1/57.3)*( (4*M(j)^2/3) + (8*M(j)^2*Cbar) -
pi*(AR*(1-beta2(k)^2)*(3+beta2(k)^2))/(beta2(k)*3*beta2(k)^2));
    end
end
fig2 = {'Mach 1', 'Mach 2', 'Mach 3', 'Mach 4'};
figure(2)
plot(beta2,CnBeta(:,1))
hold on
plot(beta2,CnBeta(:,2))
hold on
plot(beta2,CnBeta(:,3))
hold on
plot(beta2,CnBeta(:,4))
xlabel('Sideslip angle: \beta\circ', 'FontName', 'georgia');
ylabel('Yawing Moment Coefficient as a function of sideslip: C_n', 'FontName', 'georgia');
legend(fig2)
grid on
ax = gca;
ytickformat('%.4f');
% Remove exponent
ax.YAxis.Exponent = 0;
```

## C. Synthesis Appendix

Synthesis base code:

```
% SYNTHESIS BASE CODE
clc
clear
%=====
% INPUTS VARIABLES
%=====

% SWBG
Istr = 37; %[kg/m^2]
Kw = 2.7; % Wing-body
Spln = 222.6; %[m^2] -- 2396.114 ft^2
tau = 0.05;
geoOEW = [Istr,Kw,Spln];
geoOWE = [tau,Spln];

% Aero: L/D-MAX @ Mach 12 should be around 4.71
F = (tau^0.333)*(Kw^0.75);
M1 = 12;
A = 4;
B = 3;
LDMAX = (A / M1) * (M1 + B);

% Systems
Ncrw = 1; %[-]
Cun = 1.9 * 1000; %[kg]
Fmnd = 1.45 * 1000; %[ton/person]
Csys = Cun + Fmnd + Ncrw;
fsys = 0.16; %[-]
Kvv = 0.10; %[-]
```



```
Kvs = 0.02; %[-]
Vun = 5.0; %[m^3]
fcrw = 11; %[m^3/person]
Vfix = Vun + (fcrw*Ncrw);
SystemsOEW = [Csys,fsys];
SystemsOWE = [Kvv,Kvs,Vfix];

% Propulsion
TWMAX = 0.75;
WR = 3;
ETW = 11; %[kg thrust/kg weight]
Kve = 0.25 * 1000; %[ton thrust]
M = 3.2; %[-] Mach number
Ip = 107.6*(10^(-0.081*M));
rhoppl = Ip * (WR - 1);
ICI = 10 * (Ip/Istr);
propOEW = [TWMAX,WR,ETW];
propOWE = [WR,rhoppl,TWMAX,Kve];

% Mission Requirements
Wpay = 1360.777; %[kg]
Wcrew = 90.7185; %[kg/person]
Wcprv = 0.45 * 1000; %[kg/person]
Vpcrv = 6.0; %[m^3/person]
kcrw = 0.9; %[m^3/person]
Vcrw = (Vpcrv+kcrw)*Ncrw;
rhopay = 48; %[kg/m^3]
missreqOEW = [Wpay,Wcrew,Wcprv];
missreqOWE = [Ncrw,Vcrw,kcrw,Wpay,rhopay];

muATERM = 0.63;

%=====
% WEIGHT BUDGET: W_OEW
%=====

W_OEW = ((Istr*Kw*Spln) + Csys + (((TWMAX*WR)/ETW) * (Wpay+Wcrew)) + Wcprv) / ( (1/(1+muATERM)) - fsys - ((TWMAX*WR)/ETW) );

%=====
% VOLUME BUDGET: W_OWE
%=====

W_OWE = ( ((tau*(Spln^1.5))*(1-Kvv-Kvs)) - Vfix - (Ncrw*(Vcrw-kcrw)) - (Wpay/rhopay) ) / ( ((WR-1)/rhoppl) + (Kve*TWMAX*WR) );

W_OWE1 = W_OEW + Wpay + Wcrew;

%=====
% CONVERGENCE
%=====
```

## Acknowledgments

The preferred spelling of the word “acknowledgment” in American English is without the “e” after the “g.” Avoid expressions such as “One of us (S.B.A.) would like to thank...” Instead, write “F. A. Author thanks...” *Sponsor and financial support acknowledgments are also to be listed in the “acknowledgments” section.*



## References

- [1] How the X-Men's X-Jet Blackbird Compares to the SR-71. *Lockheed Martin*. <https://www.lockheedmartin.com/en-us/news/features/2017/how-the-x-men-blackbird-compares-to-the-original-sr-71.html>. Accessed Feb. 12, 2023.
- [2] Moes, T. R. *Stability and Control Estimation Flight Test Results for the SR-71 Aircraft With Externally Mounted Experiments*. National Aeronautics and Space Administration, Dryden Flight Research Center, 2002.
- [3] *Airport Master Record, Edwards AFB*. Publication FAA FORM 5010-2 (3/96). U.S. Department of Transportation Federal Aviation Administration, Edwards Air Force Base, California, 2023, p. 6.
- [4] Kucher, P. R. SR-71 Online - SR-71 Reconnaissance Profile. *SR-71 Reconnaissance Profile*. <https://www.sr-71.org/blackbird/diagrams/reconprofile.php>. Accessed Feb. 12, 2023.
- [5] Nicolai, L. M., and Carichner, G. E. *Fundamentals of Aircraft and Airship Design*. American Institute of Aeronautics and Astronautics, Inc., Reston, Virginia, 2010.
- [6] Loftin, L. K. Subsonic Aircraft: Evolution and the Matching of Size to Performance. NASA Reference Publication, Aug 01, 1980.
- [7] Chudoba, B. Parametric Sizing Process, Lab #2, MAE 4350 Aerospace Vehicle Design I. AVD Laboratory, Jan, 2023.
- [8] Ledford, T., and Harris, C. Hypersonic Convergence. Background and Methodology. Aerospace Vehicle Design (AVD) Laboratory, Feb 08, 2023.
- [9] Chudoba, B. *Stability and Control of Conventional and Unconventional Aerospace Vehicle Configurations: A Generic Approach from Subsonic to Hypersonic Speeds*. Springer International Publishing, Cham, 2019.
- [10] Coleman, G., and Chudoba, B. A Generic Stability and Control Tool for Conceptual Design, Prototype Styem Overview. In *45th AIAA Aerospace Sciences Meeting and Exhibit*, American Institute of Aeronautics and Astronautics, 2007.
- [11] Roskam, D. J. *Airplane Design Part VII: Determination of Stability, Control and Performance Characteristics*. Design, Analysis and Research Corporation, Lawrence, Kansas, 2017.
- [12] Merlin, P. W. Design and Development of the Blackbird: Challenges and Lessons Learned. Presented at the 47th AIAA Aerospace Sciences Meeting, Florida, 2009.
- [13] Mixon, B. D., and Chudoba, B. "The Lockheed SR-71 Blackbird – A Senior Capstone Re-Engineering Experience." *45th AIAA Aerospace Sciences Meeting and Exhibit, Reno, Nevada, 2007*, p. 35. <https://doi.org/10.2514/6.2007-698>.
- [14] Moes, T., Cobleigh, B., Cox, T., Conners, T., Iliff, K., and Powers, B. Flight Stability and Control and Performance Results from the Linear Aerospike SR-71 Experiment (LASRE). Presented at the 23rd Atmospheric Flight Mechanics Conference, Boston, MA, U.S.A., 1998.
- [15] Cox, T. H., and Jackson, D. Supersonic Flying Qualities Experience Using the SR-71. Presented at the Atmospheric Flight Mechanics, New Orleans, LA, 1997.
- [16] Corda, S., Moes, T. R., Mizukami, M., Hass, N. E., Jones, D., Monaghan, R. C., Ray, R. J., Jarvis, M. L., and Palumbo, N. The SR-71 Test Bed Aircraft: A Facility for High-Speed Flight Research. Jun 01, 2000.
- [17] Malvestuto, F. S., and Kuhn, R. E. *Examination of Recent Lateral-Stability-Derivative Data*. Publication NACA RM L53I08a. National Advisory Committee for Aeronautics, Washington, 1953, p. 28.
- [18] Cox, T. H., and Marshall, A. "Longitudinal Handling Qualities of the Tu-144LL Airplane and Comparisons With Other Large, Supersonic Aircraft." *National Aeronautics and Space Administration, Dryden Flight Research Center*, 2000, p. 44.
- [19] Czysz, P., Bruno, C., and Chudoba, B. *Future Spacecraft Propulsion Systems and Integration: Enabling Technologies for Space Exploration*. Springer, Berlin, Heidelberg, 2018.
- [20] Simon, S. *Development of the Vehicle Configuration Compendium: A Comprehensive Data-Information-Knowledge System to Aid in High-Speed Vehicle Design*. University of Texas at Arlington, 2022.
- [21] Anderson, J. D. *Aircraft Performance & Design*. McGraw-Hill Education, 1999.
- [22] SR-71 Online - SR-71 Flight Manual: Section 6, Page 6-2. <https://www.sr-71.org/blackbird/manual/6/6-2.php>. Accessed Feb. 18, 2023.
- [23] Yechout, T. R., Hallgren, W. F., Morris, S. L., and Bossert, D. E. *Introduction to Aircraft Flight Mechanics Performance, Static Stability, Dynamic Stability, and Classical Feedback Control*. American Institute of Aeronautics and Astronautics, Reston, UNITED STATES, 2003.
- [24] Roskam, J. *Airplane Design - Part I: Preliminary Sizing of Airplanes*. 1997.
- [25] Coleman, G. *AIRCRAFT CONCEPTUAL DESIGN – AN ADAPTABLE PARAMETRIC SIZING METHODOLOGY*. Dissertation. University of Texas at Arlington, Arlington, TX, 2010.
- [26] Gudmundsson, S. *General Aviation Aircraft Design: Applied Methods and Procedures*. Elsevier Science & Technology, Saint Louis, UNITED STATES, 2013.
- [27] Aircraft Design: A Systems Engineering Approach | Wiley. *Wiley.com*. <https://www.wiley.com/en-us/Aircraft+Design%3A+A+Systems+Engineering+Approach-p-9781119953401>. Accessed Feb. 26, 2023.
- [28] Lockheed YF-12A. *National Museum of the United States Air Force™*. <https://www.nationalmuseum.af.mil/Visit/Museum-Exhibits/Fact-Sheets/Display/Article/195777/lockheed-yf-12a/https%3A%2F%2Fwww.nationalmuseum.af.mil%2FVisit%2FMuseum-Exhibits%2FFact-Sheets%2FDisplay%2FArticle%2F195777%2Flockheed-yf-12a%2F>. Accessed Mar. 5, 2023.

 <b>PENGUIN SUPersonic</b>	<b>SENIOR DESIGN: MAE 4351 Project</b>	Ref.: MAE 4351-001-2021 Date: 19. Mar. 2023 Name: <b>Gayathri Kola</b> Status: In Progress
---	--	---

- [29] *USAF (United States Air Force) Stability and Control DATCOM (Data Compendium).*
- [30] Carpenter, B., and Docent, U. Kelly's Greatest Challenge – The Blackbirds Amazing Achievement – Visionary Tight Leadership. Washington/Northern Virginia, Nov 30, 2016.
- [31] Raymer, D. P. *Aircraft Design: A Conceptual Approach*. American Institute of Aeronautics and Astronautics, Inc, Reston, VA, 2018.
- [32] Musielak, D., Seabridge, A., Radaci, M., Marshall, D. M., Fahlstrom, P. G., Gleason, T. J., Sadraey, M. H., Gregory, J. W., Liu, T., Tewari, A., Torenbeek, E., Farokhi, S., Yedavalli, R. K., CEng, G. D. P., Kluever, C. A., Young, T. M., Keane, A. J., Sóbester, A., Scanlan, J. P., Marqués, P., and Ronch, A. D. "Scramjet Propulsion."
- [33] Roskam, J. *Airplane Design Part VIII: Airplane Cost Estimation: Design, Development, Manufacturing and Operating*. Design, Analysis and Research Corporation (DARcorporation), 2015.
- [34] DePuy, W. E., Moyer, R., Palmer, P. R., McKinney, B. J., and Kreisel, G. R. *US Military Aircraft Cost Handbook*. ANALYTIC SCIENCES CORP, Reading, Massachusetts, 1983.
- [35] Woodford, S. *The Minimisation of Combat Aircraft Life Cycle Cost through Conceptual Design Optimisation*. Ph.D. Thesis. Cranfield University, Munich, Germany, 1999.
- [36] Koelle, D. E. *Statistical-Analytical Model for Cost Estimation and Economic Optimization of Launch Vehicles*. TransCostSystems, Liebigweg, Germany.
- [37] Boren, H. E. *DAPCA A Computer Program for Determining Aircraft Development and Production Costs*. RAND Corporation, Santa Monica, California, 1967.
- [38] Carichner, G. E., and Nicolai, L. M. Fundamentals of Aircraft and Airship Design: Volume 2 - Airship Design and Case Studies. In *Fundamentals of Aircraft and Airship Design: Volume 2 - Airship Design and Case Studies*, American Institute of Aeronautics and Astronautics, Inc., 2013, p. 963.
- [39] Hildebrandt, G. G., and Sze, M. *An Estimation of USAF Aircraft Operating and Support Cost Relations*. Publication N-3062-ACQ. RAND Corporation, Santa Monica, California, 1990, p. 78.
- [40] Hess, R., and Romanoff, H. P. *Aircraft Airframe Cost Estimating Relationships Study Approach and Conclusions*. RAND Corporation, Santa Monica, California, 1987.
- [41] Sforza, P. M. *Commercial Airplane Design Principles*. Elsevier Science, 2014.